

AN ANALYSIS OF CERTAIN MATHEMATICAL ASSUMPTIONS
UNDERLYING THE DESIGN AND OPERATION OF
GAMMA-RAY SURFACE DENSITY GAGES

by

Bryant Walker Pocock

AN ABSTRACT

Submitted to Michigan State University of Agriculture
and Applied Science in partial fulfillment of
the requirements for the degree of

MASTER OF SCIENCE

Department of Agricultural Engineering

Year

1956

Approved by

Ernest H. Kidder

9/20/56

J

Since the pioneer work of Belcher, Cuykendall, and Sack at Cornell University in 1950 (1), a number of papers have appeared (2-11) describing various instruments for use in measuring densities of soil masses by means of their interactions with gamma radiation. These instruments have been either of the surface type (2) or of the depth probe type (3-11). A few such instruments have found their way into commercial availability and have met with varying degrees of success.

Without exception, all the papers describing these so-called gamma-ray density gages have indicated a need for further insight into those fundamental relationships which exist among the various parameters concerned with effective design and use of the equipment being reported. It was with the hope of filling a portion of this need that the investigation outlined in this report was conducted.

Certain mathematical relationships were assumed on theoretical grounds to exist among the several independent variables involved in the design and operation of a satisfactory gamma-ray surface density gage. These relationships were explored analytically and a number of tentative conclusions were made. On the basis of these conclusions, a gamma-ray surface density gage was designed and constructed. The performance of the gage was compared with its predicted predicted performance, and the degree of similarity between actual and predicted calibration curves was taken as justification for the original assumptions.

**AN ANALYSIS OF CERTAIN MATHEMATICAL ASSUMPTIONS
UNDERLYING THE DESIGN AND OPERATION OF
GAMMA-RAY SURFACE DENSITY GAGES**

by

Bryant Walker Pocock

A THESIS

**Submitted to Michigan State University of Agriculture
and Applied Science in partial fulfillment of
the requirements for the degree of**

MASTER OF SCIENCE

Department of Agricultural Engineering

1956

ACKNOWLEDGMENTS

The investigations reported in this thesis comprised a phase of one project in the program of research adopted by the isotopes section of the Michigan State Highway Department research laboratory on the campus of Michigan State University, in cooperation with the University of Michigan-Phoenix Memorial Project staff in Ann Arbor. The isotopes section was established in 1952 by executive order of Commissioner Charles M. Ziegler, following far-sighted recommendations by Messrs. W. W. McLaughlin and E. A. Finney, respectively testing and research engineer and director of the research laboratory of the Michigan State Highway Department, and by Dr. Henry J. Gomberg, assistant director of the Phoenix Memorial Project.

The author gratefully acknowledges his indebtedness to the following individuals for their generous assistance in the preparation of the thesis:

Professor Ernest H. Kidder, for his guidance and encouragement;

Professor George B. Beard, for checking the physical principles involved;

Professor James S. Frame and Mr. Walter E. Sommerman, for checking the mathematics;

Professor Lloyd M. Turk and Mr. E. A. Finney, for their critical reviews of the thesis;

Messrs. Ruell Ormsby and Thomas Holmes, for preparation of the art work; and

Mrs. Rosalee Burr, for typing the manuscript.

TABLE OF CONTENTS

TABLE OF CONTENTS

	PAGE
INTRODUCTION	1
THEORETICAL DEVELOPMENT	4
Preliminary Considerations	4
Attainment of Maximum Efficiency	6
Relationship of the Substrate Attenuation	
Coefficients	8
Use of the count rate meter	9
The "Count-in-Soil to Count-in-Standard" Ratio	9
The Effect of Lead Thickness	14
Equation of curve (3)	16
Equation of curve (4)	19
Equation of curve (5)	22
The magnitude of the g functions	24
Relations between curves (3), (4), and (5)	25
Determination of Source Strength	27
EXPERIMENTAL DEVELOPMENT	32
Equipment and Procedure	32
Analysis of Results	33
Equation of curve (9)	35
The magnitude of the f functions	36
A predicted calibration curve	37

DEVELOPMENT OF A GAMMA-RAY SURFACE DENSITY GAGE

BASED ON THE FOREGOING DATA	40
Construction of the Gage	40
Laboratory and Field Applications	46
SUMMARY	49
CONCLUSIONS	51
BIBLIOGRAPHY	53
APPENDIX A: GRAPHS FOR DETERMINATION OF f_1 AND f_2	
FUNCTIONS FOR CONCRETE, SAND, CLAY, AND WOOD	
SUBSTRATES	56
APPENDIX B: DATA FOR DEVELOPMENT OF EMPIRICAL	
CALIBRATION CURVE	61
APPENDIX C: CHARACTERISTICS OF SOILS USED IN	
DEVELOPMENT OF EXPERIMENTAL CALIBRATION	
CURVE	63

LIST OF TABLES

TABLE	PAGE
I. Substrate Materials Used in Experiment 1	33
II. Values of f_1 and f_2 for Substrate Materials	
Listed in Table I.	36

LIST OF FIGURES

FIGURE	PAGE
1. Effect of Lead Thickness on Activity Through the Substrate	15
2. Relation Between Total Count Rate and Rate Through Lead at Zero Thickness of Lead	31
3. Laboratory Count Rate on Concrete Substrate <u>vs</u> Thickness of Lead	34
4. f Functions <u>vs</u> Substrate Density	38
5. Theoretical Calibration Curve	39
6. Diagram of Experimental Gamma-Ray Surface Density Gage--Sheet 1	41
7. Diagram of Experimental Gamma-Ray Surface Density Gage--Sheet 2	42
8. Operator Placing Gamma-Ray Surface Density Gage for Field Determination of Soil Density	43
9. Gamma-Ray Surface Density Gage in Use for Field Determination of Soil Density.	43
10. Operator Extracting Field Soil Sample for Analysis in Laboratory	44
11. Operator Removing Soil Sample from Ground	44
12. Gamma-Ray Surface Density Gage in Use for Determination of Count Rate on Steel (Point on Experimental Calibration Curve)	45
13. Experimental Calibration Curve	48

INTRODUCTION

During the past six or seven years, several papers have appeared (1-11) describing the development of equipment for use in measuring densities of soils by means of certain interactions of gamma radiation with matter. The instruments reported in these papers have been of two types: (1) the surface gage, and (2) the depth probe.

Although the surface gage is intended for use in assessing densities near the surfaces of land masses, whereas the depth probe is designed for employment at various elevations beneath the surface, both instruments are based upon the same theory. This theory states in its simplest form that the manner in which gamma radiation interacts with matter is related to the density of the matter, that this relationship can be discovered, and that it can be used for the purpose of estimating densities with sufficient precision to be of value.

That these instruments possess both advantages and shortcomings is a fact openly conceded in all the above-mentioned reports. For example, in situ measurements are possible, yet the equipment may be expensive or difficult to procure. Determinations can be made rapidly, yet difficulties have arisen which are traceable to a lack of complete understanding of certain principles underlying the method. These principles are fundamental, and are extremely complex.

There is disagreement among the authors who have described gamma-ray density gages. Where one writer reports that they are too sensitive, another states they are not sensitive enough. Where one says the method is simple,

another says it is difficult. Four report the method to be independent of soil type, yet two others point out that the presence of rocks affects the results. Six had no comment on such an effect.

Nine authors used cobalt 60 as a source of gamma radiation, and two used radium. One used X-rays. Source strengths varied from one to seventy millicuries. Detectors employed included Geiger-Müller tubes, scintillation counters, boron 10 trifluoride tubes, X-ray film, and pocket-type ionization chambers. Two authors divided all their count rates on soil by count rates on standard concrete blocks, to eliminate the effects of changes in source strength with time. Four used fifty-five-gallon soil samples for calibration, three used samples less than fifty-five gallons, one used various quantities, and two did not report sample sizes.

Accuracies of density measurements claimed in the papers varied from plus or minus 0.5 lb/cu ft to plus or minus 5.5 lb/cu ft. Improvements suggested by the authors included use of boron-type counters and/or scintillation counters; of compact, battery-operated scalers; of smaller, or more rugged equipment; of count rate meters; and of improved designs. Suggested fields for further study embraced means for increasing sensitivity, for decreasing sensitivity, for eliminating the effect of rocks, and for limiting gamma energies; and studies of the size and shape of the field of influence and of the effect of soil moisture on density readings.

In spite of the uncertain status of the gamma-ray density gage, as is evident from the above comments, a number of these have become available commercially

--especially of the surface type--and certain supply and equipment firms are working on improved models at this date. The commercial models are expensive and have met with varying degrees of success.

A survey of the literature discloses that much remains to be done. Many refinements are needed before it can be said that a truly adequate gamma-ray surface density gage is available. Perhaps one way to approach this problem is to undertake a critical evaluation of certain basic assumptions which must be appraised before a satisfactory design can be realized.

THEORETICAL DEVELOPMENT

Preliminary Considerations

It has been shown (12, 13) that the intensity, A_x , of gamma radiation penetrating an absorber varies closely in accordance with the relation,

$$A_x = A_0 e^{-\mu x}, \quad (1)$$

where A_0 is the intensity at zero thickness of absorber,

μ is the total attenuation coefficient of absorber,

and

x is the thickness of absorber.

The degree of precision with which a Geiger-Müller tube can be used to measure the term, A , in equation (1) will depend to some extent upon the constants or parameters associated with the experiment in question.

Conventional gamma-ray surface density gages which have been described (2) make use of a lead absorber, which separates the source from the counter tube. This assembly is placed in contact with some material such as soil, the density of which is to be measured. The substrate material actually comprises an additional absorber in parallel with, and beneath the lead. The total radiation received by the counter tube is that which is reflected by and transmitted through both the lead and the substrate. It obviously becomes of importance to create a design capable of distinguishing minute differences in substrate density most efficiently, yet with minimum weight. Usually the density range of interest is not large.

Since in general the activity detected through the substrate only, for a given thickness of lead between source and counter tube, is a function of the density of the substrate and of the strength and energy of the source, this activity may be given closely by the relation,

$$A_s = g(D, E) A \frac{f_1(D, E)}{e^{f_2(D, E) x}}, \quad (2)$$

where E is source energy.

For a given source energy, equation (2) becomes

$$A_s = g(D) A \frac{f_1(D)}{e^{f_2(D) x}}, \quad (3)$$

where A_s is the activity through the substrate only, of density, D, at thickness of lead absorber, x;

$g(D)$ is the coefficient of reflection of the substrate, always positive;

$f_1(D)$ is the log scattering ratio of the substrate, always positive;

$f_2(D)$ is the negative total attenuation coefficient of the substrate;

and

A is the activity through the lead only at zero thickness of lead (a function of source strength).

The total intensity, A_t , received by the counter tube then will be the sum of that through the substrate and that through the lead absorber; or,

$$A_t = g(D) A \frac{f_1(D)}{e^{f_2(D) x}} + A e^{-\mu x} \quad (4)$$

It is desirable to compare the activities scattered by and transmitted through substrates of two different densities, $D = D_1$ and $D = D_2$, where $D_1 < D_2$. Experimental evidence shows that when $D_1 < D_2$, $A_{s1} > A_{s2}$ within the limits of this discussion. Exceptions to the general statement will appear subsequently (Figure 13).

For $D = D_1$,

$$A_{s1} = g_1 A e^{f_{11} + f_{21}x}, \quad (5)$$

where g_1 is $g(D_1, E)$,

f_{11} is $f_1(D_1, E)$, and

f_{21} is $f_2(D_1, E)$.

For $D = D_2$,

$$A_{s2} = g_2 A e^{f_{12} + f_{22}x}, \quad (6)$$

where g_2 is $g(D_2, E)$,

f_{12} is $f_1(D_2, E)$, and

f_{22} is $f_2(D_2, E)$.

Attainment of Maximum Efficiency

In order that a surface density gage operate with maximum efficiency within the range of densities between D_1 and D_2 , inclusive, it is necessary to maximize the extent of ΔA_g within this density range. A suitable parameter for this purpose consists of the independent variable, x .

$$\Delta A_s = A_{s1} - A_{s2} = g_1 A^{f_{11}} e^{f_{21}x} - g_2 A^{f_{12}} e^{f_{22}x}.$$

Letting

$$a = g_1 A^{f_{11}},$$

$$u = e^{f_{21}x},$$

$$b = g_2 A^{f_{12}}, \text{ and}$$

$$c = \frac{f_{22}}{f_{21}} > 1 \quad (\text{to be shown}),$$

then

$$\Delta A_s = au - bu^c,$$

$$(\Delta A_s)_u = a - bcu^{c-1}, \text{ and}$$

$$(\Delta A_s)_{uu} = -bc(c-1)u^{c-2} < 0.$$

Therefore

$$(\Delta A_s)_u = a - bcu^{c-1} = 0 \tag{7}$$

is a maximum. From this,

$$u^{c-1} = \frac{a}{bc},$$

$$u = \left(\frac{a}{bc} \right)^{\frac{1}{c-1}}, \text{ and}$$

$$x = \ln \left[\left(\frac{a}{bc} \right)^{\frac{f_{21}}{c-1}} \right]$$

$$\begin{aligned}
&= \ln \left[\frac{\frac{1}{f_{21} - f_{22}} \quad \frac{f_{12} - f_{11}}{f_{21} - f_{22}}}{\left(\frac{f_{22}g_2}{f_{21}g_1} \right) A} \right] \\
&= \frac{\ln \left[\frac{f_{12} - f_{11}}{(f_{22}g_2 / f_{21}g_1) A} \right]}{f_{21} - f_{22}} \quad (8)
\end{aligned}$$

Equation (8) gives the value, x , of that thickness of lead which will provide maximum ΔA_s within any given range of substrate densities. It is a most useful relation. It will be referred to henceforth as $x_{(opt)}$.

Relationship of the Substrate Attenuation Coefficients

It is also instructive to develop the relation which exists between the activities, A_{s1} and A_{s2} , and the total linear attenuation coefficients of the two substrate materials concerned at the value of x , $x = x_{(opt)}$.

$$\begin{aligned}
\frac{A_{s1}}{A_{s2}} &= \frac{a}{b} u^{1-c} \\
&\quad \frac{1}{c-1} \\
\text{At} \quad u &= \left(\frac{a}{bc} \right), \\
\frac{A_{s1}}{A_{s2}} &= \frac{a}{b} \left(\frac{a}{bc} \right)^{-1} = c = \frac{f_{22}}{f_{21}} \quad (9)
\end{aligned}$$

Equation (9) states that when the thickness, x , of absorber separating the source from the counter is so chosen that the difference between the activity through a substrate only, of density, $D = D_1$, and that through a substrate only, of density,

$D = D_2$, is at a maximum ($x = x_{(opt)}$), the ratio of the activities through the substrates is equal to the reciprocal of the ratio of the total linear attenuation coefficients of the two substrate materials. It is significant that this relation holds true only for $x = x_{(opt)}$.

It can be seen from equation (9) that the ratio of activities through any two substrates of different densities is a constant with respect to source strength at $x = x_{(opt)}$, although the value of $x_{(opt)}$ will vary according to equation (8). Equation (8) contains an A term, thus causing $x_{(opt)}$ to be partially dependent upon source strength.

Use of the count rate meter. It is of interest at this point that such a ratio of two different activities through substrate materials of different densities can be measured most efficiently with a count rate meter possessing a linear scale only when the latter is adjusted to read the greater activity at the upper limit of its scale. Comparisons between activities at other scale settings diminish in precision as the highest reading falls below the upper scale limit. These considerations, in addition to the generally low order of precision of rate meters and the difficulty of applying statistical treatments to data derived with their use, quite definitely indicate the superiority of scaling equipment where small differences in density must be determined.

The "Count-in-Soil to Count-in-Standard" Ratio

The U. S. Army Corps of Engineers, in their Field Tests of Nuclear Instruments for the Measurement of Soil and Density (6), report (page 10) that a "count-

in-soil to count-in-standard ratio is used to eliminate variations in count that may be caused by changes in . . . source strength." The Cornell group (1) and (2) also reported results based on the ratio of activity through an unknown substrate to activity through a standard substrate. Both groups used cobalt 60 as a source of gamma radiation.

It is important to examine the validity of the use of a "count-in-soil to count-in-standard" ratio. Changes in source strength are due to the effect of half-life only, although changes in observed count rate may be a result also of background changes. If the effects of all these changes could be eliminated by the use of a standard, as suggested, this might well avoid the necessity for making periodic calibrations of equipment.

Equations (5) and (6) may be employed to yield activities through an unknown substrate, A_{s1} , and through a standard substrate, A_{s2} . Use of the ratio, $\frac{A_{s1}}{A_{s2}}$, leads to equation (9), as shown, provided $x = x_{(opt)}$. At other values of the term, x , use of the ratio results in the following equation:

$$\frac{A_{s1}}{A_{s2}} = \frac{g_1}{g_2} A^{(f_{11} - f_{12})} e^{(f_{21} - f_{22})x} . \quad (10)$$

Since the value of A will change with time as a function of the half-life of the source used,

$$A_{t2} = A_{t1} e^{-\lambda t} , \quad (11)$$

where λ is the decay constant of the source (12, 13).

Upon substitution in equation (10) of the expression for A_{t2} obtained from equation (11), the ratio becomes,

$$\frac{A_{s1}}{A_{s2}} = \frac{g_1}{g_2} A_{t1}^{(f_{11} - f_{12})} e^{\left[(f_{11} - f_{12})(-\lambda t) + (f_{21} - f_{22})x \right]}. \quad (12)$$

It is possible to consider the significance of the ratio expressed in equation (12) under three sets of conditions, as follows.

Condition (1). $D_{s1} = D_{s2}$. Under this condition, the ratio

$$\frac{A_{s1}}{A_{s2}} = 1.$$

Therefore, where the density of the sample is equal to that of the standard, the value of the term, t , in equation (12) is without effect, and the consequence of half-life on the calibration curve is eliminated. This condition, however, is not attainable in practice.

Condition (2). $D_{s1} > D_{s2}$. Under this condition,

$$f_{11} > f_{12}.$$

Therefore,

$$(f_{11} - f_{12})(-\lambda t) < 0,$$

and the effect of the value of the term, t , in equation (12) must be to reduce the value of the ratio as the magnitude of t increases.

Condition (3). $D_{s1} < D_{s2}$. Under this condition,

$$f_{11} < f_{12}.$$

Therefore,

$$(f_{11} - f_{12})(-\lambda t) > 0,$$

and the effect of the value of the term, t , in equation (12) must be to increase the value of the ratio as the magnitude of t increases.

As a result of these considerations, it becomes apparent that use of the "count-in-soil to count-in-standard" ratio will not eliminate the effect on the calibration curve of half-life in reducing source strength in practice. Yet, although use of the ratio will not eliminate the effect of half-life, it is possible that its use may reduce this effect. It is of value to examine this possibility more closely.

The relative effect of time on the calibration curve can be ascertained by examining the relative magnitudes of the coefficients of the term, t , in equation (12), and in equation (5) modified by substitution of the expression for A_{t2} from equation (11). It can be shown for all three possible density relations listed above under conditions (1) through (3) that

$$|(f_{11} - f_{12})(-\lambda)| < |(-f_{11} \lambda)|.$$

Therefore, the effect on the calibration curve of reduction of source strength with time as a function of half-life is lessened by use of the "count-in-soil to count-in-standard" ratio, although this effect is not eliminated except where $D_{s1} = D_{s2}$.

It is also important to examine the possibility that use of the $\frac{A_{s1}}{A_{s2}}$ ratio may be of advantage in eliminating variations in observed count rates due to changes in background activity. Where

A_1 is observed count rate in excess of background activity, B_1 , and

A_2 is observed count rate in excess of background activity, B_2 ,

$$\frac{A_1 + B_1}{A_2 + B_1} = C_1, \text{ and}$$

$$\frac{A_1 + B_2}{A_2 + B_2} = C_2.$$

It is apparent mathematically that where $A_1 \neq A_2$

$$C_1 \neq C_2, \text{ unless}$$

$$B_1 = B_2.$$

Therefore, use of the ratio does not eliminate the necessity of subtracting background activities in practice.

It appears from the above equations and inequalities that use of the ratio, $\frac{A_{s1}}{A_{s2}}$, for the purpose of lessening the effect on the calibration curve of reduction of source strength with time as a function of half-life is justifiable on theoretical grounds. The standard employed should have a density as nearly as possible equal to the average density of the substrates being studied; or, if the range of substrate densities is large, several standards should be employed. It should be emphasized

that use of the ratio will not eliminate the need for recalibration, but will merely serve to reduce the required frequency of recalibration. With long-lived sources such as cesium 137, use of the ratio does not appear justifiable, as one would be undertaking a daily burden in order to lessen the frequency of a semiannual or annual one.

The Effect of Lead Thickness

From the above equations, it is possible to plot $\ln A_s$ vs x , as in Figure 1, which shows activity through the substrate only as a function of the thickness of absorber separating the source from the counter tube. Curves (1) and (1a) are for the minimum substrate density within the range of interest, and curves (2) and (2a) are for the maximum substrate density within that range. Curves (1) and (2) are for a source, (a), producing an activity, A_1 , and curves (1a) and (2a) are for a source, (b), producing an activity, A_2 .

The antilog length of V_1 gives the greatest absolute difference between curves (1) and (2), hence maximum ΔA_s for these curves, and its x-ordinate states the optimum absorber thickness for the given range of densities using source (a). Similarly, the antilog length of V_2 gives the greatest absolute difference between curves (1a) and (2a), hence maximum ΔA_s for these curves, and its x-ordinate states the optimum absorber thickness for the same range of densities using source (b). Sources (a) and (b) vary in strength only.

Curve (3) has the property that $A_{s1} = A_{s2}$. All curves of the type (1), (1a), etc., intersect with corresponding curves of the type (2), (2a), etc.,

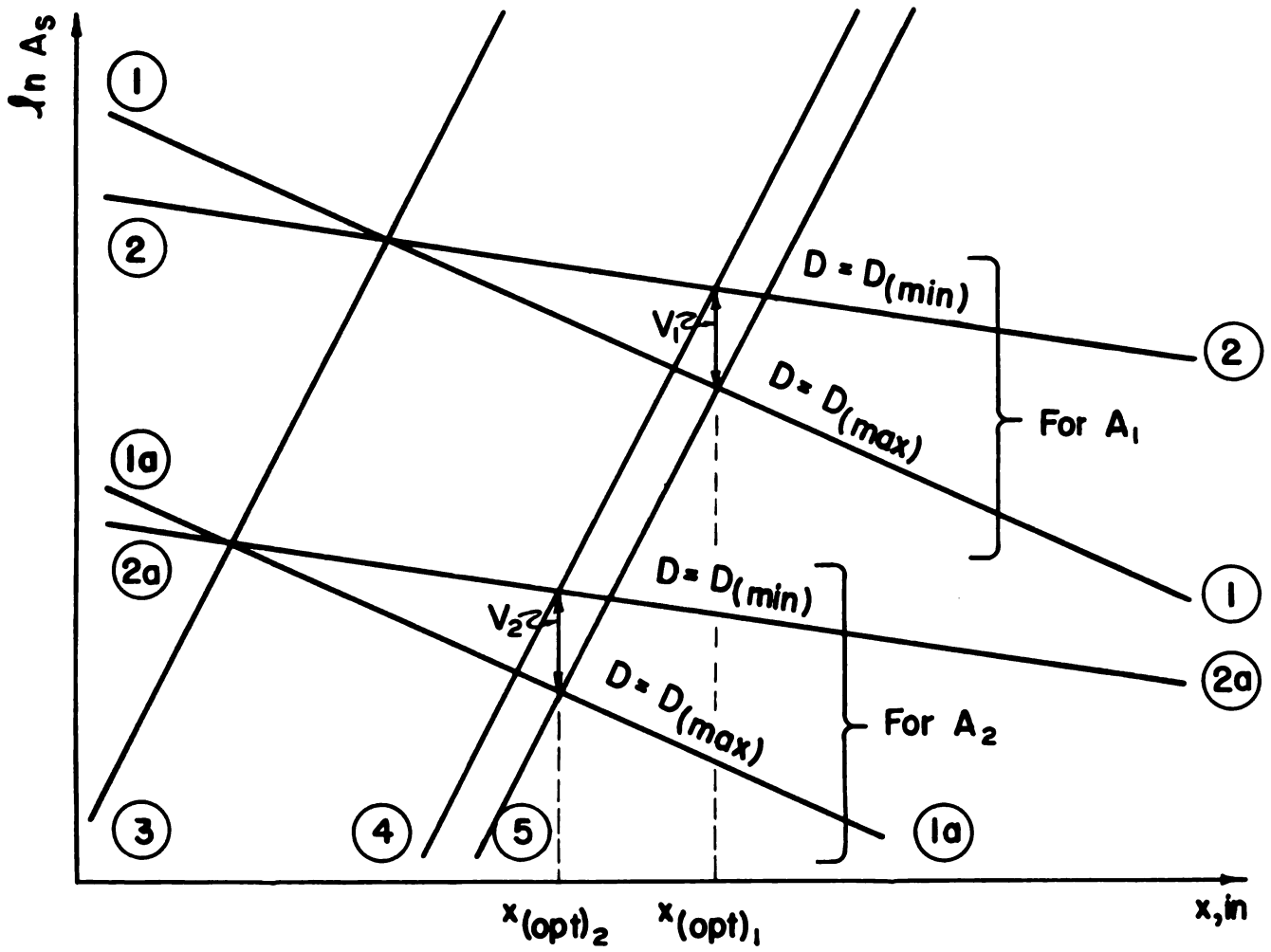


Figure 1. Effect of lead thickness on activity through the substrate.

along curve (3) . Curve (4) contains all values of A_{s1} for which A is maximum and D is minimum within the given range of substrate densities, x being equal to $x_{(opt)}$. Curve (5) contains all values of A_{s2} for which A is minimum and D is maximum within the given range of substrate densities, x being equal to $x_{(opt)}$. The equations for curves (1) and (2) are equations (5) and (6), respectively, which are also valid for curves (1a) and (2a) , etc.

Equation for curve (3) . The equation for curve (3) may be developed as follows.

$$A_{s1} = A_{s2} .$$

Therefore,

$$g_1 A \frac{f_{11}}{e} \frac{f_{21} x}{e} = g_2 A \frac{f_{12}}{e} \frac{f_{22} x}{e} ,$$

$$A \frac{f_{11}}{e} = \left(\frac{g_2}{g_1} \right) A \frac{f_{12}}{e} \frac{(f_{22} - f_{21}) x}{e} ,$$

$$A^{(f_{11} - f_{12})} = \left(\frac{g_2}{g_1} \right) e^{(f_{22} - f_{21}) x} , \text{ and}$$

$$A = \left(\frac{g_2}{g_1} \right)^{\left(\frac{1}{f_{11} - f_{12}} \right)} e^{\left(\frac{f_{22} - f_{21}}{f_{11} - f_{12}} \right) x} . \quad (13)$$

Substitution in equation (5) of the value of A obtained from equation (13) gives the relation,

$$A_{s1} = g_1 \left(\frac{g_2}{g_1} \right)^{\left(\frac{f_{11}}{f_{11} - f_{12}} \right)} e^{\left\{ x \left[f_{21} + f_{11} \left(\frac{f_{22} - f_{21}}{f_{11} - f_{12}} \right) \right] \right\}}, \quad (14)$$

which is one form of the equation for curve (3). The term,

$$g_1 \left(\frac{g_2}{g_1} \right)^{\left(\frac{f_{11}}{f_{11} - f_{12}} \right)},$$

gives the ordinate of curve (3) at $x = x_0$, or its intersection with the $\ln A_s$ -axis.

The term,

$$f_{21} + f_{11} \left(\frac{f_{22} - f_{21}}{f_{11} - f_{12}} \right),$$

gives the slope of curve (3).

Substitution in equation (6) of the value of A obtained from equation (13)

gives the relation,

$$A_{s2} = g_2 \left(\frac{g_2}{g_1} \right)^{\left(\frac{f_{12}}{f_{11} - f_{12}} \right)} e^{\left\{ x \left[f_{22} + f_{12} \left(\frac{f_{22} - f_{21}}{f_{11} - f_{12}} \right) \right] \right\}}, \quad (15)$$

which is another form of the equation for curve (3). The term,

$$g_2 \left(\frac{g_2}{g_1} \right)^{\left(\frac{f_{12}}{f_{11} - f_{12}} \right)},$$

likewise gives the ordinate of curve (3) at $x = x_0$, or its intersection with the \ln

A_s -axis, and the term,

$$f_{22} + f_{12} \left(\frac{f_{22} - f_{21}}{f_{11} - f_{12}} \right) ,$$

gives its slope. Hence, if $A_{s1} = A_{s2}$, the terms for intersection and slope contained in equations (14) and (15) must be identities.

In order to show that the terms for intersection are identical,

$$1 \equiv 1;$$

Therefore,

$$\frac{f_{11} - f_{12}}{f_{11} - f_{12}} \equiv 1,$$

$$\frac{f_{11}}{f_{11} - f_{12}} \equiv 1 + \frac{f_{12}}{f_{11} - f_{12}} ,$$

$$\left(\frac{f_{11}}{f_{11} - f_{12}} \right) \ln \frac{g_2}{g_1} \equiv \ln \frac{g_2}{g_1} + \left(\frac{f_{12}}{f_{11} - f_{12}} \right) \ln \frac{g_2}{g_1} ,$$

$$\left(\frac{f_{11}}{f_{11} - f_{12}} \right) \ln \frac{g_2}{g_1} \equiv \ln g_2 - \ln g_1 + \left(\frac{f_{12}}{f_{11} - f_{12}} \right) \ln \frac{g_2}{g_1} ,$$

$$\ln g_1 + \left(\frac{f_{11}}{f_{11} - f_{12}} \right) \ln \frac{g_2}{g_1} \equiv \ln g_2 + \left(\frac{f_{12}}{f_{11} - f_{12}} \right) \ln \frac{g_2}{g_1} ,$$

$$\ln \left[g_1 \left(\frac{g_2}{g_1} \right)^{\left(\frac{f_{11}}{f_{11} - f_{12}} \right)} \right] \equiv \ln \left[g_2 \left(\frac{g_2}{g_1} \right)^{\left(\frac{f_{12}}{f_{11} - f_{12}} \right)} \right] , \text{ and}$$

$$g_1 \left(\frac{g_2}{g_1} \right) \left(\frac{f_{11}}{f_{11} - f_{12}} \right) = g_2 \left(\frac{g_2}{g_1} \right) \left(\frac{f_{12}}{f_{11} - f_{12}} \right) .$$

Therefore, the intersections are identical.

In order to show that the terms for slope are identical,

$$1 = 1 ,$$

$$\frac{f_{21}f_{11} - f_{21}f_{12} + f_{11}f_{22} - f_{11}f_{21}}{f_{11} - f_{12}} = \frac{f_{22}f_{11} - f_{22}f_{12} + f_{12}f_{22} - f_{12}f_{21}}{f_{11} - f_{12}} ,$$

$$f_{21} + f_{11} \left(\frac{f_{22} - f_{21}}{f_{11} - f_{12}} \right) = f_{22} + f_{12} \left(\frac{f_{22} - f_{21}}{f_{11} - f_{12}} \right) .$$

Therefore, the slopes are identical. Since both intersections and slopes are identical, equations (14) and (15) are identical and are in fact, singly or together, the equation of curve (3) .

Equation for curve (4) . The equation for curve (4) may be developed as follows. Substitution in equation (9) of the expression for A_{s1} derived in equation (5), and of the expression for A_{s2} derived in equation (6), yields the relation,

$$\frac{g_1 A_{s1}^{f_{11}} e^{f_{21} x_{(opt)}}}{g_2 A_{s2}^{f_{12}} e^{f_{22} x_{(opt)}}} = \frac{f_{22}}{f_{21}} , \text{ whence}$$

$$\frac{g_1}{g_2} A_{s1}^{(f_{11} - f_{12})} e^{(f_{21} - f_{22}) x_{(opt)}} = \frac{f_{22}}{f_{21}} ,$$

$$A^{(f_{11} - f_{12})} = \left(\frac{f_{22}}{f_{21}} \right) \left(\frac{g_2}{g_1} \right) e^{(f_{22} - f_{21})x_{(opt)}}, \text{ and}$$

$$A = \left(\frac{f_{22}g_2}{f_{21}g_1} \right) e^{\left(\frac{1}{f_{11} - f_{12}} \right) \left[\frac{(f_{22} - f_{21})x_{(opt)}}{f_{11} - f_{12}} \right]}. \quad (16)$$

Substitution in equation (5) of the expression for A derived from equation (16) shows that

$$A_{S1} = g_1 \left(\frac{f_{22}g_2}{f_{21}g_1} \right) \left(\frac{f_{11}}{f_{11} - f_{12}} \right) e^{\left\{ \left[f_{21} + f_{11} \left(\frac{f_{22} - f_{21}}{f_{11} - f_{12}} \right) \right] x_{(opt)} \right\}}. \quad (17)$$

Equation (17) is the equation of curve (4). The term,

$$g_1 \left(\frac{f_{22}g_2}{f_{21}g_1} \right) \left(\frac{f_{11}}{f_{11} - f_{12}} \right),$$

gives the intersection of curve (4) with the $\ln A_S$ -axis. The slope of curve (4) is given by the term,

$$f_{21} + f_{11} \left(\frac{f_{22} - f_{21}}{f_{11} - f_{12}} \right).$$

Since the intersection of curve (4) with the $\ln A_S$ -axis is less in magnitude than the intersection of curve (3),

$$g_1 \left(\frac{f_{22}g_2}{f_{21}g_1} \right) \left(\frac{f_{11}}{f_{11} - f_{12}} \right) \text{ must } < g_1 \left(\frac{g_2}{g_1} \right) \left(\frac{f_{11}}{f_{11} - f_{12}} \right) .$$

It will be instructive to show analytically that this is true.

By definition,

$$g_1 > 0 .$$

Therefore, g_1 cancels, and the sense of the inequality remains the same. As will be shown in inequality (24) ,

$$f_{12} > f_{11} > 0 .$$

Therefore,

$$\frac{f_{11}}{f_{11} - f_{12}} < 0 ,$$

this term cancels, and the sense of the inequality is reversed:

$$\frac{g_2}{g_1} < \frac{f_{22}g_2}{f_{21}g_1} .$$

By definition,

$$g_2 > 0 . \text{ Therefore,}$$

$$\frac{f_{22}}{f_{21}} > 1 . \tag{18}$$

By definition,

$$f_{21} < 0 . \text{ Therefore,}$$

$$f_{22} < f_{21}, \text{ and} \tag{19}$$

$$g_1 \left(\frac{f_{22}g_2}{f_{21}g_1} \right) \left(\frac{f_{11}}{f_{11} - f_{12}} \right) \text{ must } < g_1 \left(\frac{g_2}{g_1} \right) \left(\frac{f_{11}}{f_{11} - f_{12}} \right) .$$

Equation for curve (5) . The equation for curve (5) may be developed as follows. Substitution in equation (6) of the expression for A derived from equation (16) shows that

$$A_{s2} = g_2 \left(\frac{f_{22}g_2}{f_{21}g_1} \right) \left(\frac{f_{12}}{f_{11} - f_{12}} \right) e^{\left\{ \left[f_{22} + f_{12} \left(\frac{f_{22} - f_{21}}{f_{11} - f_{12}} \right) \right] x_{(opt)} \right\}} . (20)$$

Equation (20) is the equation of curve (5) . The term,

$$g_2 \left(\frac{f_{22}g_2}{f_{21}g_1} \right) \left(\frac{f_{12}}{f_{11} - f_{12}} \right) ,$$

gives the ordinate of curve (5) at $x = x_0$, or its intersection with the $\ln A_s$ -axis.

The slope of curve (5) is given by the term,

$$f_{22} + f_{12} \left(\frac{f_{22} - f_{21}}{f_{11} - f_{12}} \right) .$$

Since the intersection of curve (5) with the $\ln A_s$ -axis is less in magnitude than the intersection of curve (4) ,

$$g_2 \left(\frac{f_{22}g_2}{f_{21}g_1} \right) \left(\frac{f_{12}}{f_{11} - f_{12}} \right) \text{ must } < g_1 \left(\frac{f_{22}g_2}{f_{21}g_1} \right) \left(\frac{f_{11}}{f_{11} - f_{12}} \right) .$$

It will be instructive to show analytically that this is true.

As will be shown in inequality (24),

$$(f_{11} - f_{12}) < 0.$$

Therefore,

$$g_2 \left(\frac{f_{22}g_2}{f_{21}g_1} \right)^{f_{12}} > g_1 \left(\frac{f_{22}g_2}{f_{21}g_1} \right)^{f_{11}}, \text{ and}$$

$$\frac{g_2}{g_1} \left(\frac{f_{22}g_2}{f_{21}g_1} \right)^{(f_{12} - f_{11})} > 1.$$

Recalling from inequality (18) that

$$\frac{f_{22}}{f_{21}} > 1,$$

and anticipating, as will be shown in inequality (24), that

$$f_{12} > f_{11},$$

and recalling that by definition

$$f_{12} > 0 \text{ and}$$

$$f_{11} > 0 \text{ and}$$

$$(f_{12} - f_{11}) > 0,$$

it follows that

$$\left(\frac{f_{22}}{f_{21}} \right)^{(f_{12} - f_{11})} > 1. \quad (21)$$

At this point, it is convenient to let

$$\left(\frac{f_{22}}{f_{21}} \right)^{(f_{12} - f_{11})} = Z .$$

As shown,

$$Z > 1 .$$

Therefore,

$$\begin{aligned} \frac{g_2}{g_1} \left(\frac{f_{22}g_2}{f_{21}g_1} \right)^{(f_{12} - f_{11})} &= Z \left(\frac{g_2}{g_1} \right)^{[(f_{12} - f_{11}) + 1]} > 1 , \\ \left(\frac{g_2}{g_1} \right)^{[(f_{12} - f_{11}) + 1]} &> Z^{-1} , \text{ and} \\ \frac{g_2}{g_1} &> Z^{\left(\frac{-1}{f_{12} - f_{11} + 1} \right)} > 0 . \end{aligned} \tag{22}$$

Therefore,

$$g_2 \left(\frac{f_{22}g_2}{f_{21}g_1} \right)^{\left(\frac{f_{12}}{f_{11} - f_{12}} \right)} < g_1 \left(\frac{f_{22}g_2}{f_{21}g_1} \right)^{\left(\frac{f_{11}}{f_{11} - f_{12}} \right)} .$$

The magnitude of the g functions. It may be shown that inequality (22) will hold true if it be assumed that

$$\frac{g_2}{g_1} = 1 ,$$

as follows.

As shown,

$$1 < Z .$$

Therefore,

$$1 = 1^{(f_{12} - f_{11} + 1)} > Z^{-1} > 0 , \text{ and}$$

$$1 > Z^{\left(\frac{-1}{f_{12} - f_{11} + 1} \right)} > 0 .$$

Therefore, inequality (22) holds true if $\frac{g_2}{g_1} = 1$.

Recalling that by definition,

$$g_1 > 0 , \text{ and}$$

$$g_2 > 0 ,$$

$$0 \text{ may } < \frac{g_2}{g_1} \text{ may } < 1 ,$$

but this would not satisfy all possible values of Z . Therefore, where the values of g_1 and g_2 are not known, although there is nothing to indicate that

$$\frac{g_2}{g_1} \text{ cannot } > 1 ,$$

inequality (22) is always satisfied by the assumption that

$$g_1 = g_2 = 1 . \quad (23)$$

Relations between curves (3) , (4) , and (5) . Since the intersection of curve (5) with the $\ln A_g$ -axis is less than that of curve (3) ,

$$g_2 \left(\frac{f_{22}g_2}{f_{21}g_1} \right) \left(\frac{f_{12}}{f_{11} - f_{12}} \right) < g_1 \left(\frac{g_2}{g_1} \right) \left(\frac{f_{11}}{f_{11} - f_{12}} \right) .$$

Therefore,

$$\begin{aligned} & \left(\frac{f_{12}}{f_{11} - f_{12}} \right) \left(\frac{f_{12}}{f_{11} - f_{12}} \right) \left(\frac{f_{11}}{f_{11} - f_{12}} \right) \\ & \left(\frac{g_2}{g_1} \right) \left(\frac{f_{22}}{f_{21}} \right) \left(\frac{g_2}{g_1} \right) < \left(\frac{g_2}{g_1} \right) , \text{ and} \\ & \left(\frac{f_{22}}{f_{21}} \right) \left(\frac{f_{12}}{f_{11} - f_{12}} \right) < 1 . \end{aligned}$$

Since, as shown in inequality (18),

$$\begin{aligned} \frac{f_{22}}{f_{21}} & > 1 , \\ \left(\frac{f_{12}}{f_{11} - f_{12}} \right) & < 0 . \end{aligned}$$

Since, by definition,

$$\begin{aligned} f_{11} & > 0 , \text{ and} \\ f_{12} & > 0 , \\ (f_{11} - f_{12}) & < 0 . \end{aligned}$$

Therefore,

$$f_{11} < f_{12} . \quad (24)$$

Comparisons of equations (14), (15), (17), and (18) show that the slopes of curves (3), (4), and (5) are equal; therefore, the curves are parallel on semi-logarithmic coordinate paper.

Determination of Source Strength

In order to obtain the maximum counting rate with available equipment, it is necessary to consider the rate through the lead absorber and the rate through the substrate material. The rate through the lead is established by the term,

$$A e^{-\mu x},$$

where μ is the total attenuation coefficient of lead, and x is the thickness of lead. The rate through a substrate material of density, $D = D_{(\min)}$ in the range of interest (so that A_g is maximum within this range), is given by the term,

$$g_1 A e^{f_{11} f_{21} x},$$

in which x is that thickness of lead absorber, $x = x_{(\text{opt})}$, which will provide maximum ΔA_g within the density range. The total count rate, A_t , is given by the relation,

$$\begin{aligned}
& -\mu \ln \left[\left(\frac{f_{22}g_2}{f_{21}g_1} \right) \left(\frac{1}{f_{21}-f_{22}} \right) \left(\frac{f_{12}-f_{11}}{f_{21}-f_{22}} \right) \right]_A \\
& + g_1 A e^{f_{11}} f_{21} \ln \left[\left(\frac{f_{22}g_2}{f_{21}g_1} \right) \left(\frac{1}{f_{21}-f_{22}} \right) \left(\frac{f_{12}-f_{11}}{f_{21}-f_{22}} \right) \right]_A = \\
& t = A e
\end{aligned}$$

$$\begin{aligned}
& \ln \left[\left(\frac{f_{22}g_2}{f_{21}g_1} \right) \left(\frac{-\mu}{f_{21}-f_{22}} \right) \left[\frac{-\mu(f_{12}-f_{11})}{f_{21}-f_{22}} \right]_A \right] \\
& + g_1 A e^{f_{11}} \ln \left[\left(\frac{f_{22}g_2}{f_{21}g_1} \right) \left(\frac{f_{21}}{f_{21}-f_{22}} \right) \left[\frac{f_{21}(f_{12}-f_{11})}{f_{21}-f_{22}} \right]_A \right] = \\
& A e
\end{aligned}$$

Therefore,

$$\begin{aligned}
 A_t = & \underbrace{\left(\frac{f_{22}g_2}{f_{21}g_1} \right) \left[\frac{-\mu}{f_{21}-f_{22}} \right] A}_{\text{Term 1}} + \underbrace{g_1 \left(\frac{f_{22}g_2}{f_{21}g_1} \right) \left(\frac{f_{21}}{f_{21}-f_{22}} \right) A}_{\text{Term 2}} + \underbrace{\left[f_{11} + \frac{f_{21}(f_{12}-f_{11})}{f_{21}-f_{22}} \right] A}_{\text{Term 3}}, \quad (25)
 \end{aligned}$$

$$A_t = A_x + A_{sx},$$

where $x = x_{(opt)}$.

It is seen that equation (25) is the equation of a curve, (6), which is the sum of two separate curves, (7) and (8). These curves can be plotted on logarithmic coordinate paper, as shown in Figure 2. In the case of curves (7) and (8), the coefficient gives the intersection with the $\ln A_t$ -axis at $A = 1$, and the exponent gives the slope.

Once a value of A_t has been selected as convenient for the equipment to be used, the value of A for this value of A_t at $x = x_{(opt)}$ can be read from the graph. To determine the indicated source strength to be used, this value of A should be divided by the efficiency of the detection unit in the geometry under consideration. It should be emphasized that the value of μ in equation (25) has been modified by varying the source-counter distance, and must be determined by experiment.

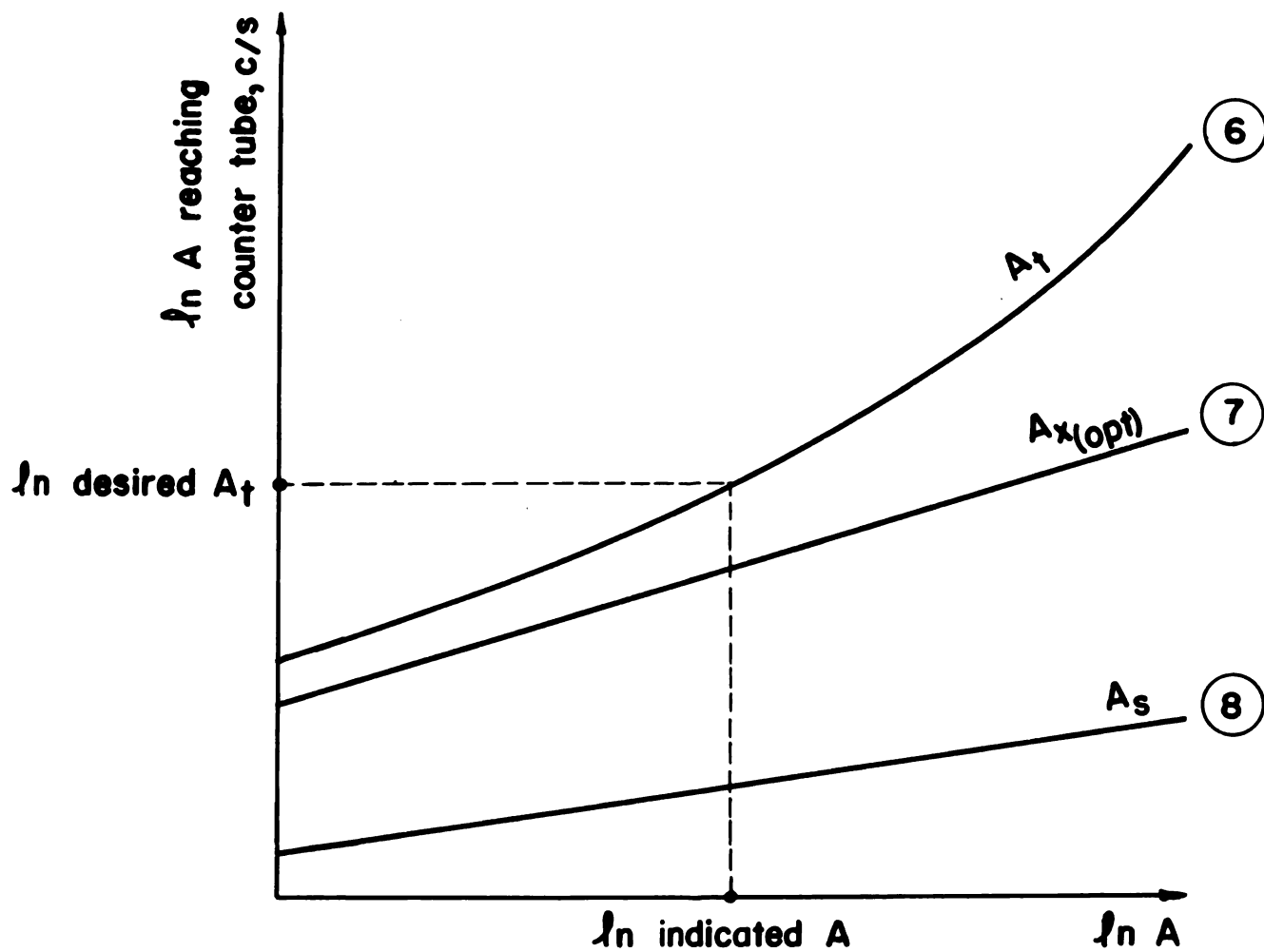


Figure 2. Relation between total count rate and rate through lead at zero thickness of lead.

EXPERIMENTAL DEVELOPMENT

Equipment and Procedure

A series of laboratory experiments was designed in order to evaluate the optimum thickness of lead absorber, $x_{(opt)}$; the magnitude of the functions, f_{11} , f_{21} , f_{12} , and f_{22} ; and the amount of the activity A . A nominally five-millicurie sealed cesium 137 source was purchased, to be used in conjunction with a TGC 2 GM counter tube. It was decided to evaluate $x_{(opt)}$ within the range of substrate densities between 60 and 180 lb/cu ft, inclusive.

A number of three-inch by nine-inch by one-eighth-inch lead plates were prepared, for use as separators between the source and the counter tube. The assembly was mounted on a forty-inch by fourteen-inch by three-quarter-inch plywood base in such a manner that the number of lead plates, standing upright on their long edges between the source and the counter, could be varied.

Rather than keep the source-to-counter distance constant for all numbers of lead absorber plates, this distance was allowed to change with the total lead thickness. In this way, for each thickness of lead, the typical geometry of a gamma-ray surface density gage containing that thickness of lead absorber was approximated. In all cases, provision was made for packing the sandwich of lead plates together as tightly as possible without introducing extraneous reflecting materials. The thickness of the plywood base, constant throughout the experiment, was neglected.

Samples of substrate materials of different bulk densities were provided, contained in wood boxes possessing more than infinite volume for the field of influence employed, upon which the assembly could be placed for obtaining count rates at various thicknesses of lead absorber. Background activities were subtracted from gross activities in all cases. Total counts ranged from $N = 16,000$ to $N = 256,000$, depending upon the count rate. Substrate materials used included those shown in Table I.

TABLE I
SUBSTRATE MATERIALS USED IN EXPERIMENT 1

Material	Bulk density, lb/cu ft
Concrete	150.2
Sand	93.8
Clay	63.09
Wood	29.2

Analysis of Results

For each determination, net activity in counts per second was plotted on semilogarithmic coordinate paper against total thickness of lead absorber in inches, as shown in Figure 3 for a concrete substrate. That portion of the curve (9) which is a straight line (above approximately two and one-quarter inches of lead) was interpreted as the curve of A_s including negligible quantities of A_x . The difference between its extrapolation and the balance of the curve below approximately two and one-quarter inches of lead (curve 10) was interpreted to be the curve of A_x only.

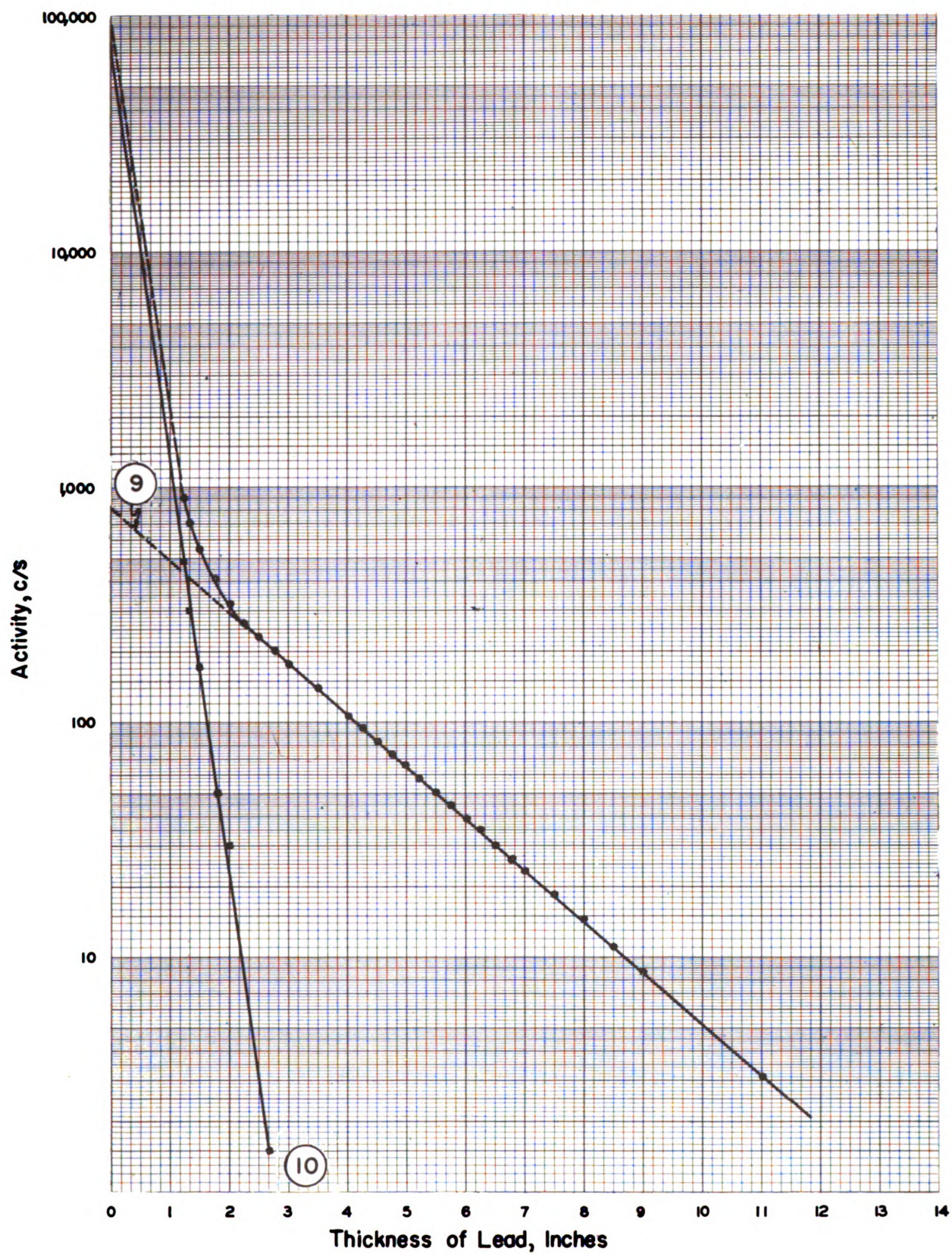


Figure 3. Laboratory count rate on concrete substrate vs thickness of lead.

The intersection of curve (10) with the $\ln A$ -axis gives the magnitude of A for the substrate used. This value was found to be 79,000 counts per second in the case of all substrate materials listed in Table I.

The intersection of curve (9) extrapolated to the $\ln A$ -axis gives the magnitude of A_s at $x = 0$ (activity through the substrate only at zero thickness of lead) for the substrate used. The value of A_s at $x = 0$ varied with the substrate material, being 790 counts per second in the case of concrete, 568 in the case of sand, 410 in the case of clay, and 198 in the case of wood.

The fact that curve (9) has a straight-line portion above x equals approximately two and one-quarter inches of lead when plotted on semilogarithmic coordinate paper effectively precludes the possibility that equation (2) have an x -term in its first term, either as a coefficient of or as an exponent of A .

Equation of curve (9). For the purpose of developing the equation of curve (9), equation (3) can be written,

$$A_s = A^{\frac{f_1}{1}} e^{\frac{f_2}{2} x}, \quad (26)$$

which is the equation of curve (9).

When $x = 0$, the intersection of curve (9) with the $\ln A$ -axis may be determined by the relation,

$$\ln A_s = \ln A^{\frac{f_1}{1}}. \quad (27)$$

The slope of curve (9) is given by the term, f_2 .

The magnitude of the f functions. It can be seen from equation (27) that at $x = 0$,

$$f_1 = \frac{\ln A_s}{\ln A} \quad (28)$$

Therefore, in the case of concrete substrate,

$$f_1 = \frac{\ln 790}{\ln 79,000} = 0.5916, \quad (29)$$

and the value of f_2 may be determined between any two points, as, for example, $x = 6$ and $x = 8.7$. Then,

$$f_2 = \frac{2.30259 - 3.66356}{2.7} = -0.5040 \quad (30)$$

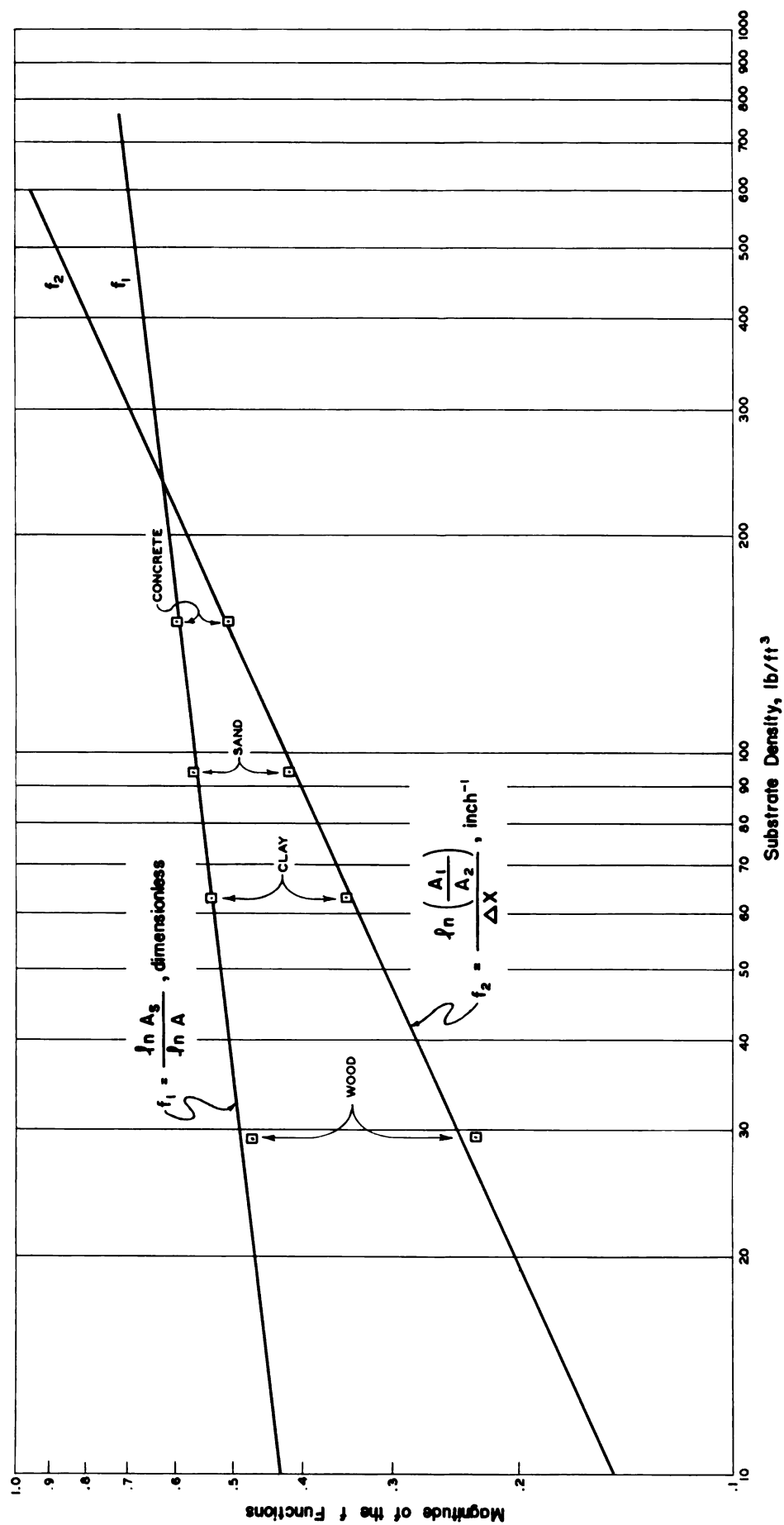
Similarly, curves corresponding to curve (9) for a concrete substrate may be plotted from data derived from use of the other substrate materials listed in Table I. The values of the functions, f_1 and f_2 , calculated from these data in a manner similar to that outlined in equations (29) and (30), are given in Table II.

TABLE II
VALUES OF f_1 AND f_2 FOR SUBSTRATE
MATERIALS LISTED IN TABLE I

Material	f_1	f_2
Concrete	0.5916	-0.5040
Sand	0.5623	-0.4115
Clay	0.5334	-0.3442
Wood	0.4689	-0.2290

A predicted calibration curve. The values of the functions, f_1 and f_2 , shown in Table II were plotted on logarithmic coordinate paper against the bulk densities of the substrate materials from which they were derived, as shown in Figure 4. It will be noted that the values of f_1 and f_2 for wood fall slightly below their corresponding curves, a fact which may be attributed to the probability that the volume of the wood sample used was insufficiently infinite for the geometry employed.

The curves for f_1 and f_2 in Figure 4 were used to obtain values for these functions at other densities, in order to establish a quasi-theoretical calibration curve for an instrument designed on the basis of the above data. This predicted calibration curve is shown in Figure 5. Data for deriving the curve are available in the Appendix.

Figure 4. f functions vs substrate density

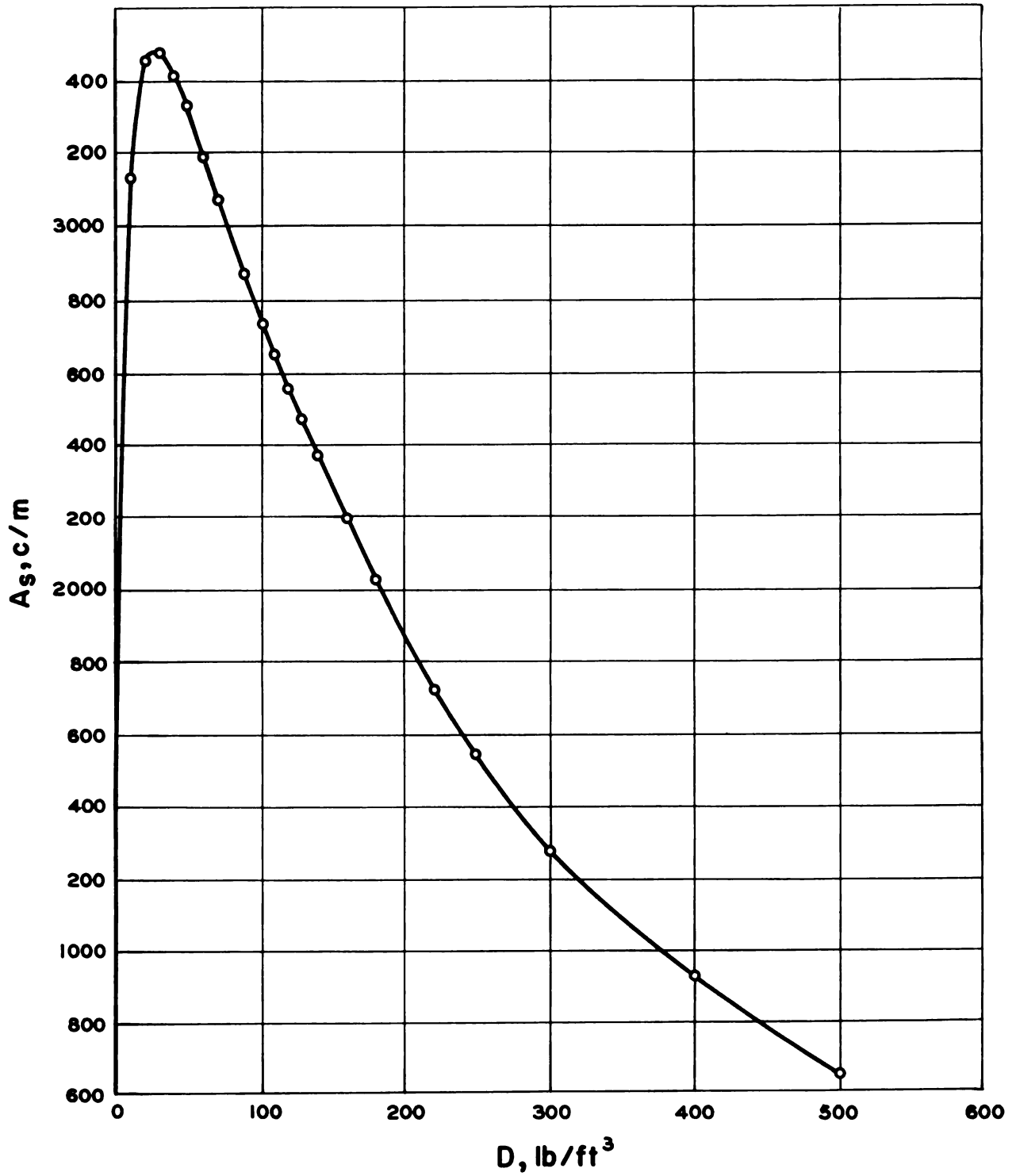


Figure 5. Predicted calibration curve based on $A_s = gA \frac{f_1(D)}{e^{f_2(D) \times 60}}$

$$= \left(79,000 \frac{f_1(D)}{e^{6 f_2(D)}} \right) 60$$

DEVELOPMENT OF A GAMMA-RAY SURFACE DENSITY GAGE

BASED ON THE FOREGOING DATA

Construction of the Gage

After substitution of the values of f_{11} and f_{21} at $D = 60$ pounds per cubic foot and of the values of f_{12} and f_{22} at $D = 180$ pounds per cubic foot, taken from the f_1 and f_2 curves of Figure 4, it was found from equation (8) that the magnitude of $x_{(opt)}$ was 6.348 inches using the five-millicurie source of cesium 137. However, an accurate plot of Figure 1 showed that the magnitude of ΔA_g at $x = 6.000$ inches was 17.0 counts per second, compared with a magnitude of 17.1 counts per second at $x = 6.348$ inches. This difference in magnitude of ΔA_g , therefore, was only 0.58 per cent of its magnitude at $x = x_{(opt)}$. By accepting a value of 6.000 inches for $x_{(opt)}$, it was found that a saving of 5.482 per cent could be realized in the weight of the lead absorber.

Accordingly, a gage was designed on the basis that $x_{(opt)} = 6.0$ inches, as illustrated in Figures 6 through 12, using the nominally five-millicurie sealed cesium 137 source of gamma radiation. Housing for the assembly was constructed of twenty-eight-gage monel metal arranged in the shape of a box with a sliding, removable cover. Total weight of the gage was ten pounds.

As shown in the photographs (Figures 8, 9, and 11) a two-wheel dolly was constructed to accommodate the scaling equipment. Accessibility of a truck containing a 110-volt, 3500-watt AC power supply made the equipment sufficiently mobile for

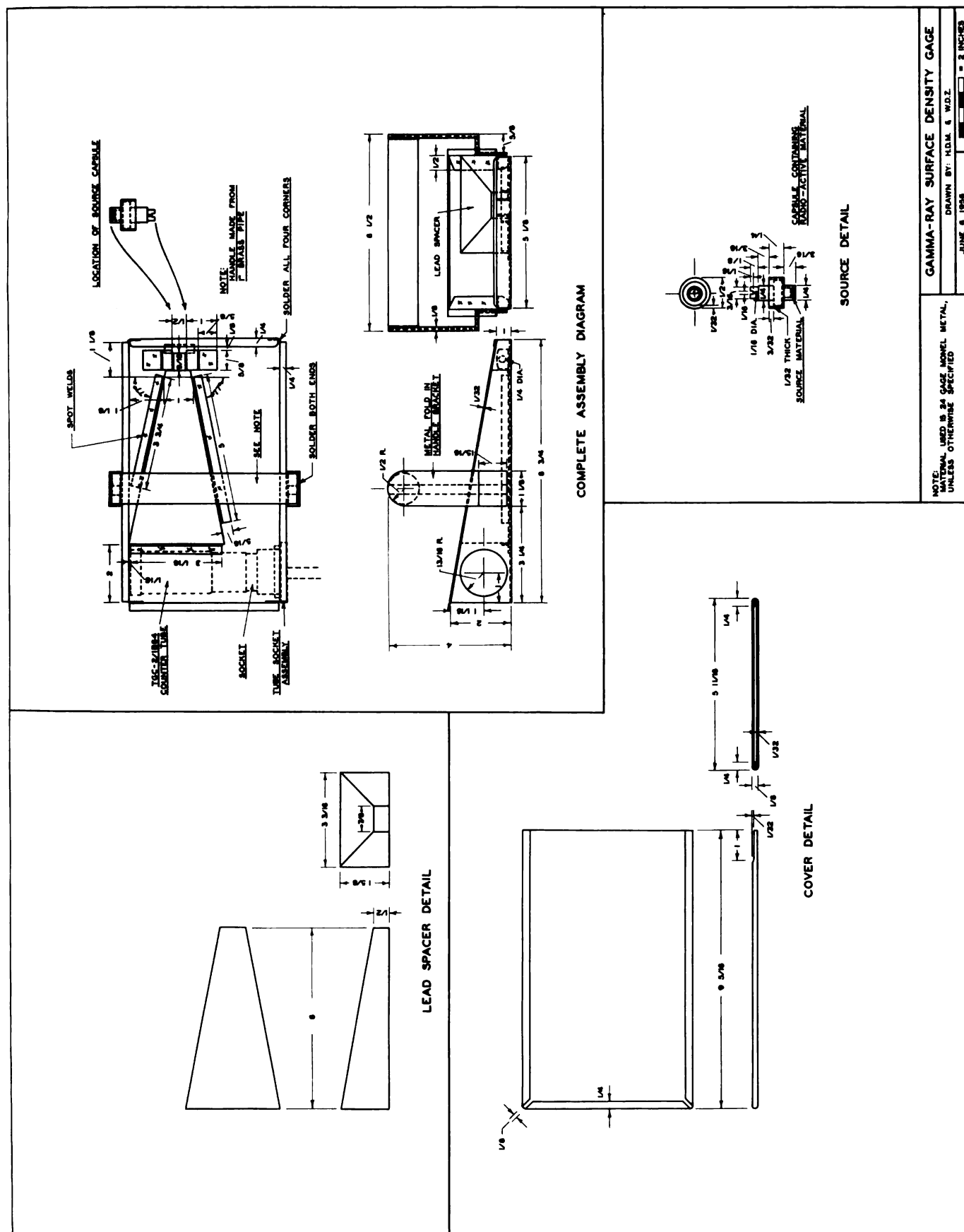
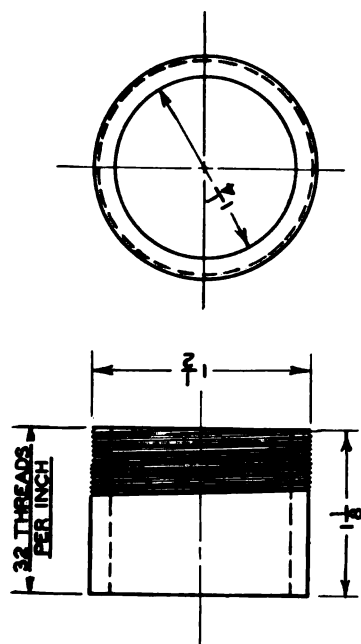
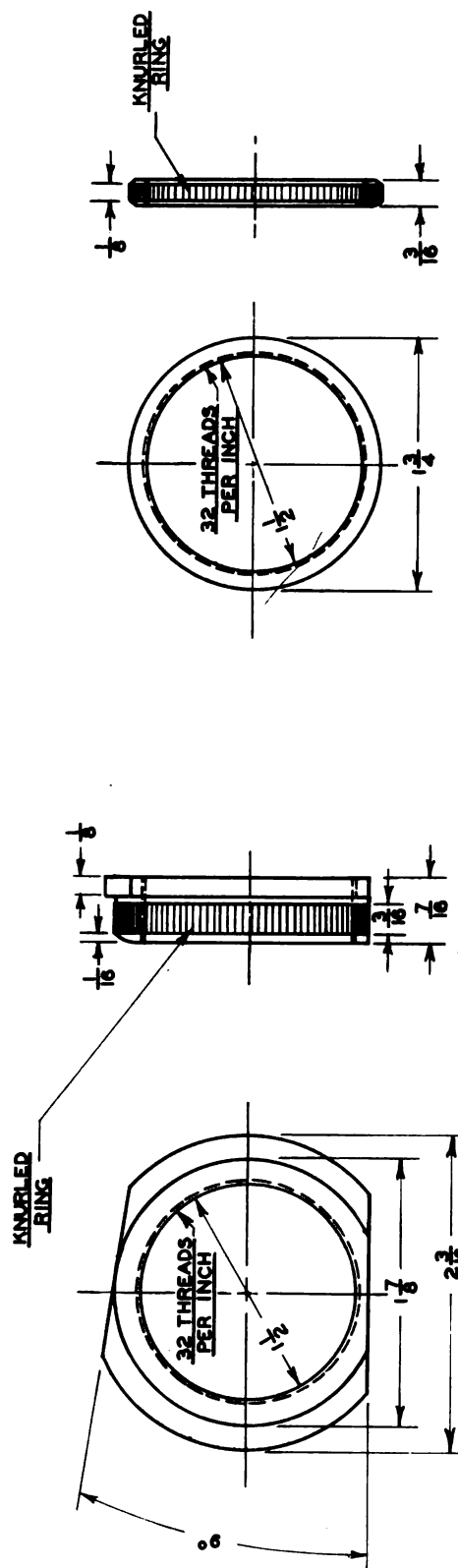


Figure 6. Gamma-Ray Surface Density Gage



SOCKET CONNECTING SLEEVE



NOTE:
SOCKET ASSEMBLY USED
ON 4-PIN TUBE SOCKET

TUBE SOCKET ASSEMBLY

DRAWN BY: W. D. Z.

JUNE 9, 1956

1 INCH

Figure 7. Tube Socket Assembly.



Figure 8. Operator placing gamma-ray surface density gage for field determination of soil density.



Figure 9. Gamma-ray surface density gage in use for field determination of soil density.



Figure 10. Operator extracting field soil sample for analysis in laboratory.



Figure 11. Operator removing soil sample from ground.

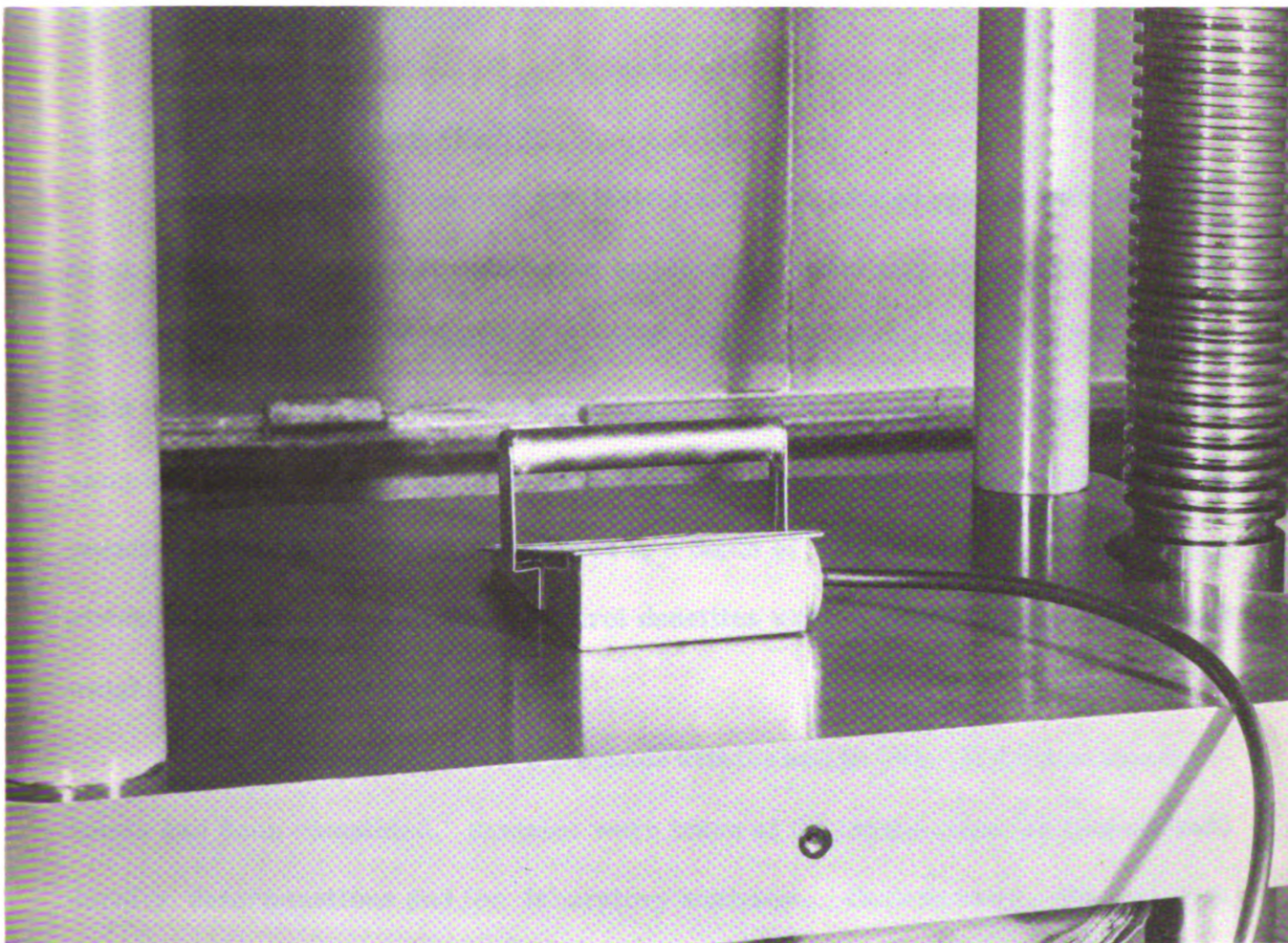


Figure 12. Gamma-ray surface density gage in use for determination of count rate on steel (point on experimental calibration curve).

field use. A cord length of ten feet was used between the TGC 2 counter tube and the Nuclear model 183 scaler.

Laboratory and Field Applications

Count rates obtained with the instrument were plotted against bulk densities for a number of materials. Substrates employed included air, wood shavings, wood boards, paper (stacks of identical journals), concrete, steel, and lead; and various soils under several degrees of compaction. The soils included laboratory and field samples. In the laboratory, they were contained in wood boxes measuring twenty by twenty-four inches. These were filled to a depth of approximately six inches and struck off flush with the tops. Control densities were determined by volume and weight measurements on a wet basis.

Field gage measurements were made with the soil in situ. After gage measurements had been completed, samples were taken at the same sites for conventional density determinations and for laboratory analyses. Occasionally, the soil was tamped, and both types of density determination were repeated to evaluate the effect of tamping on soil compaction. It was found that tamping increased the density of soil No. 21 by approximately sixteen pounds per cubic foot.

Conventional density determinations made at the site were based on volume-weight relationships taken immediately, by use of a portable balance and the so-called "can" technique. Both tops and bottoms were removed from twelve-ounce number one cans, and one end of each can was ground sharp. It was found possible

to insert the can into the soil with minimum disturbance to a depth of four inches (the depth of the field of influence of the density gage in soil) and to extract a sample of sufficient size for independent determinations. By striking the soil off at the bottom of the can with a sharp knife, a right cylinder could be produced, whose height could easily be determined. The volumes of less cohesive soils were measured by filling the cavity with uniformly graded Ottawa sand.

Figure 13 shows the calibration curve for the density gage based upon experimental determinations in the laboratory and in the field. It can be seen that this curve agrees fairly well with the theoretical calibration curve shown in Figure 5. The degree of similarity between the two curves is an indication of the degree of validity of the basic assumptions contained in equation (2) with respect to the developments here reported.

Experimental evidence indicated, as noted above, that the depth of the field of influence in soils was about four inches. In concrete, the depth was three and one-half inches, and in air it was about twenty inches. A procedure adopted for plotting points on the experimental calibration curve consisted of referring all count rates to a selected count rate with the gage suspended in air. The selected rate in air included the background rate at the time it was determined. As subsequent determinations in air fell above or below the selected rate, due to variations in background activity, all other rates on substrates determined at approximately the same time were raised or lowered accordingly.

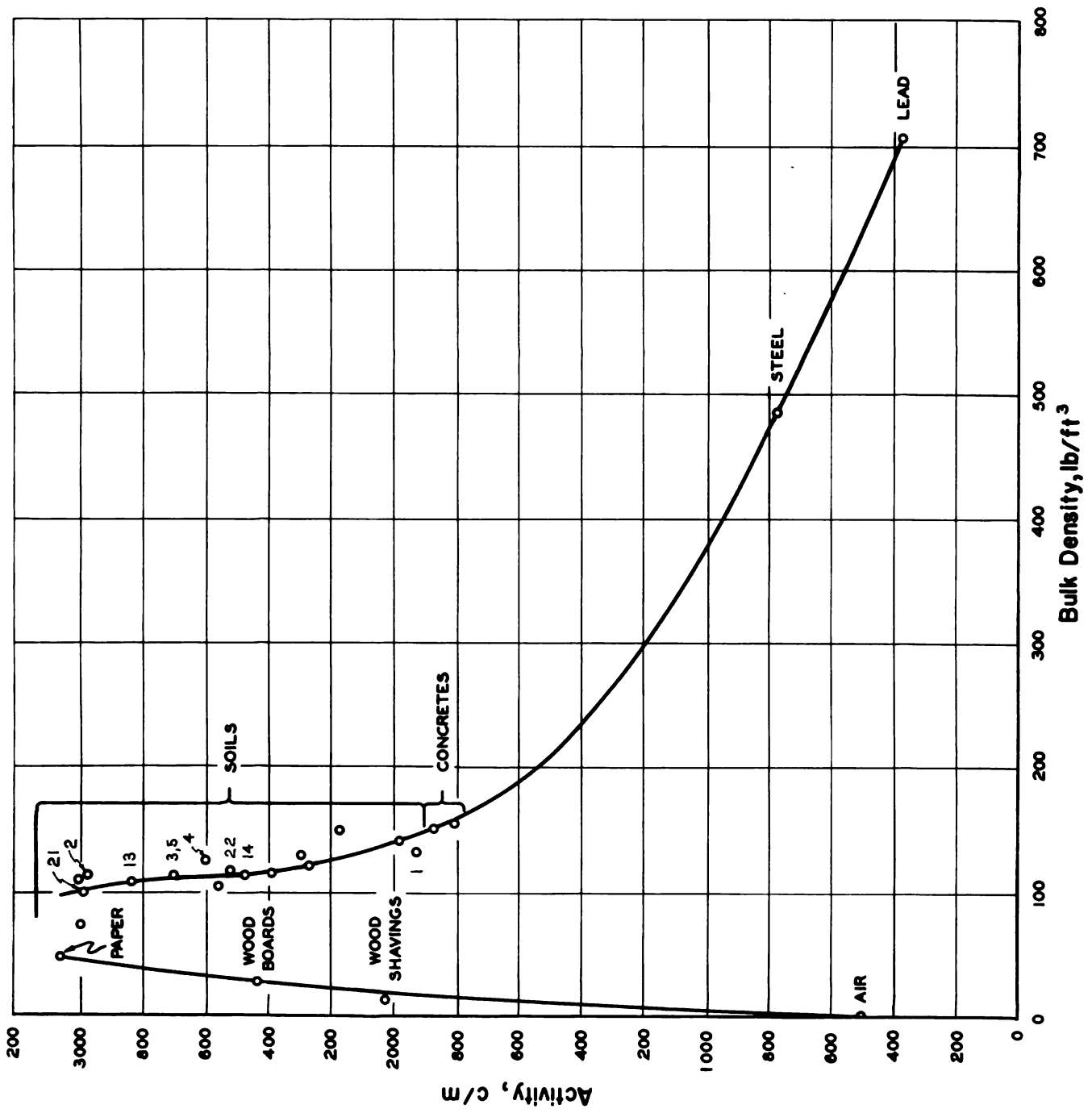


Figure 13. Experimental calibration curve

SUMMARY

A survey of the literature on the development of the gamma-ray density gage disclosed a variety of conflicting reports. Investigators disagreed as to the best design, the best type and strength of source, the extent of the field of influence, the effect of soil type, the ease of making determinations, the sensitivity of the method, and the use of reference standards. As a result of the survey, it was felt that a fundamental approach to the entire subject would have to be considered.

Certain basic assumptions were made on theoretical grounds only, related to known interactions of gamma radiation with matter. An equation was developed from these assumptions and subjected to rigorous treatment. Expressions were obtained stating the best thickness of lead absorber, the relation between density and total linear attenuation coefficient, certain limitations on the use of standards, and the effect of source strength. The magnitudes of certain functions contained in the equation were measured experimentally, and a predicted calibration curve was established for a gamma-ray surface density gage designed on the basis of the equation.

A gage was constructed, based upon the fundamental assumptions, designed to operate most efficiently within a range of densities between 60 and 180 pounds per cubic foot. A nominally five-millicurie sealed source of cesium 137 was used in the gage, separated from a TGC 2 counter tube by 6.0 inches of lead. Weight of the gage was ten pounds.

The gage was used to measure densities of various materials which ranged in bulk density from that of air to that of lead. The experimental calibration curve for the instrument was compared with the predicted calibration curve, and the extent of similarity between the two curves was taken as indicative of the degree of validity of the assumptions underlying the fundamental equation.

CONCLUSIONS

It would appear on the basis of experimental evidence cited that the following conclusions are justified:

1. Information of assistance in the designing of a satisfactory gamma-ray surface density gage can be obtained by the assumption that

$$A_s = g(D, E) A \frac{f_1(D, E)}{e} \frac{f_2(D, E)}{e} x \quad (2)$$

2. The best thickness of lead absorber separating the source and Geiger-Müller counter tube of a gamma-ray surface density gage is given by the relation,

$$x_{(opt)} = \frac{\ln \left[\frac{(f_{22}g_2/f_{21}g_1) A}{f_{21} - f_{22}} \right]}{f_{21} - f_{22}} \quad (8)$$

For a gage employing five millicuries of cesium 137 and a TGC 2 Geiger-Müller counter tube, the value of $x_{(opt)}$ is 6.348 inches when the gage is intended to operate at maximum efficiency within a range of densities between 60 and 180 pounds per cubic foot.

3. The ratio of activities through any two substrates of different densities, when optimum thickness of lead absorber is used, is equal to the reciprocal of the ratio of the total linear attenuation coefficients of the two substrate materials. This relation holds true at no other thickness of lead.

4. Use of a "count-in-soil to count-in-standard" ratio will not eliminate the necessity of subtracting background count rates, nor the need for periodic recalibrations of a gamma-ray surface density gage; it will merely serve to reduce the required frequency of recalibration. Use of such a ratio is not justified with long-lived sources of gamma radiation. Its use with short-lived and medium-lived isotopes is of questionable value.

5. The indicated source strength to be employed can be determined by dividing the value of A by the efficiency of the detection unit in the geometry to be used. The required value of A can be read directly from a plot of A_t vs A (Figure 2), where the value of $A_{(tot)}$ represents the desired maximum total count rate for the instrument.

6. Rate meters employing linear scales can be used with maximum efficiency in conjunction with gamma-ray surface density gages only if adjusted so that, when comparing the densities of two materials, the greater activity is read at the upper scale limit. The superiority of scaling equipment over count rate meters for use with density gages appears to be indicated.

7. The need for a commercially available, portable, battery-operated scaler of modest cost and of rugged, though light, design is definitely indicated.

BIBLIOGRAPHY

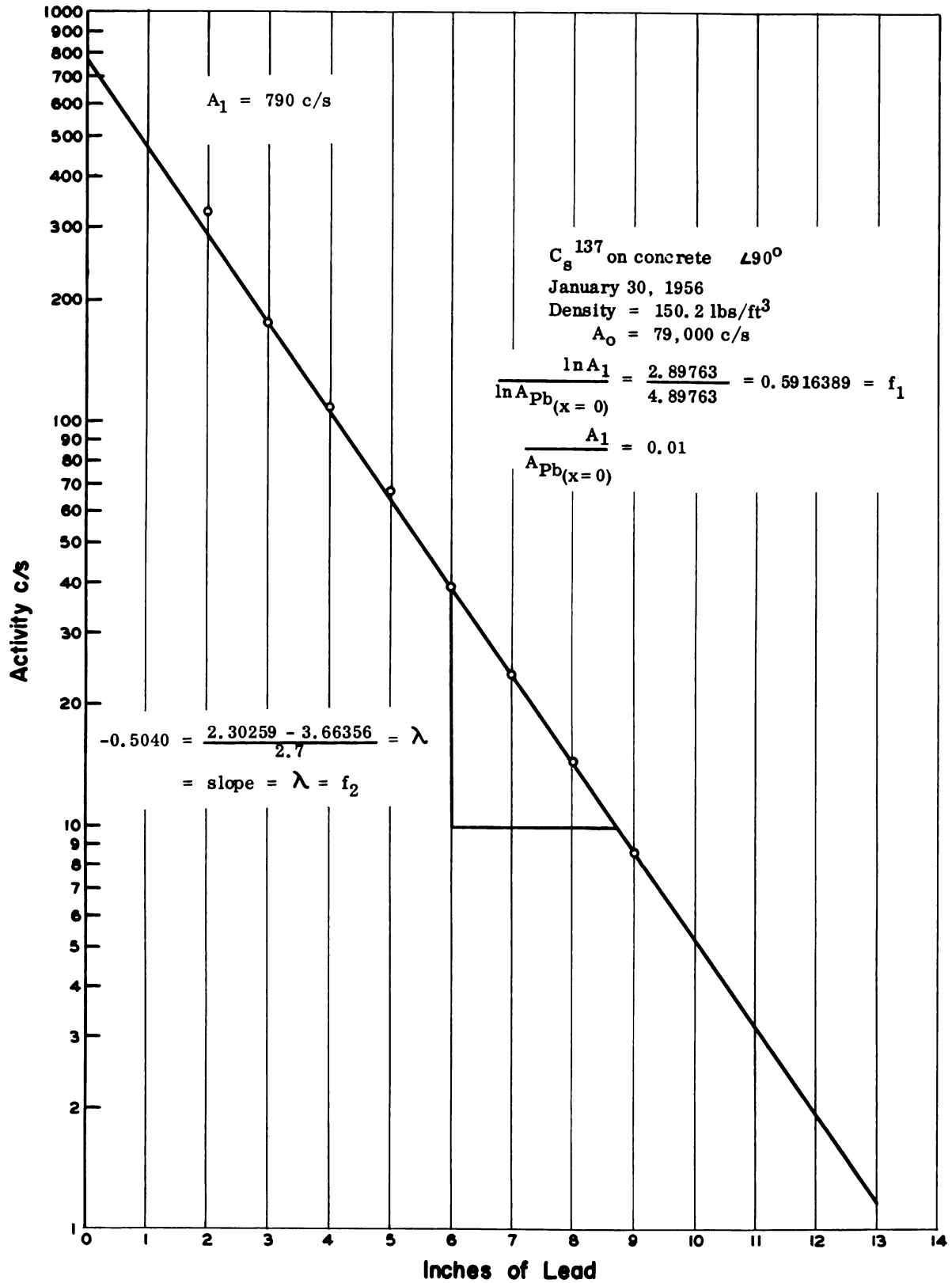
1. Belcher, D. J.; Cuykendall, T. R.; and Sack, H. S.; The Measurement of Soil Moisture and Density by Neutron and Gamma Ray Scattering. Technical Development Report No. 127, Civil Aeronautics Administration Technical Development and Evaluation Center, Indianapolis, Indiana, October, 1950.
2. Belcher, D. J.; Cuykendall, T. R.; and Sack, H. S.; Nuclear Meters for Measuring Soil Density and Moisture in Thin Surface Layers. Technical Development Report No. 161, Civil Aeronautics Administration Technical Development and Evaluation Center, Indianapolis, Indiana, February, 1952.
3. Carlton, Paul F.; Belcher, D. J.; Cuykendall, T. R.; and Sack, H. S.; Modifications and Tests of Radioactive Probes for Measuring Soil Moisture and Density. Technical Development Report No. 194, Civil Aeronautics Administration Technical Development and Evaluation Center, Indianapolis, Indiana, March, 1953.
4. Vomocil, J. A., "In Situ Measurement of Soil Bulk Density," Agricultural Engineering, Vol. 35, No. 9, September, 1954, pp. 651-4.
5. Berdan, D.; and Bernhard, R. K.; Pilot Studies of Soil Density Measurements by Means of X-Rays. Presented at the Fifty-third Annual Meeting of the American Society for Testing Materials, June 26-30, 1950.
6. U.S. Army Corps of Engineers, Field Tests of Nuclear Instruments for the Measurement of Soil Moisture and Density. Miscellaneous Paper No. 4-117, Vicksburg Infiltration Project, Forest Service, U.S. Department of Agriculture, for Waterways Experiment Station, Vicksburg, Mississippi, March, 1955.
7. Hosticka, Harold E.; "Radioisotopes and Nuclear Reactions Applied to Soil Mechanics Problems," Symposium on the Use of Radioisotopes in Soil Mechanics, ASTM Special Technical Publication No. 134, American Society for Testing Materials. Presented at a meeting of Committee D-18 on Soils for Engineering Purposes, Cleveland, Ohio, March 5, 1952.
8. Bernhard, R. K.; and Chasek, M.; Soil Density Determination by Direct Transmission of Gamma Rays. Presented at the Fifty-eighth Annual Meeting of the American Society for Testing Materials, June 26-July 1, 1955; 18 pp.
9. Miles, M. E.; Energy Distribution of Gamma Rays Scattered Around a Soil Density Probe. Master's Thesis, Cornell University, June, 1952.

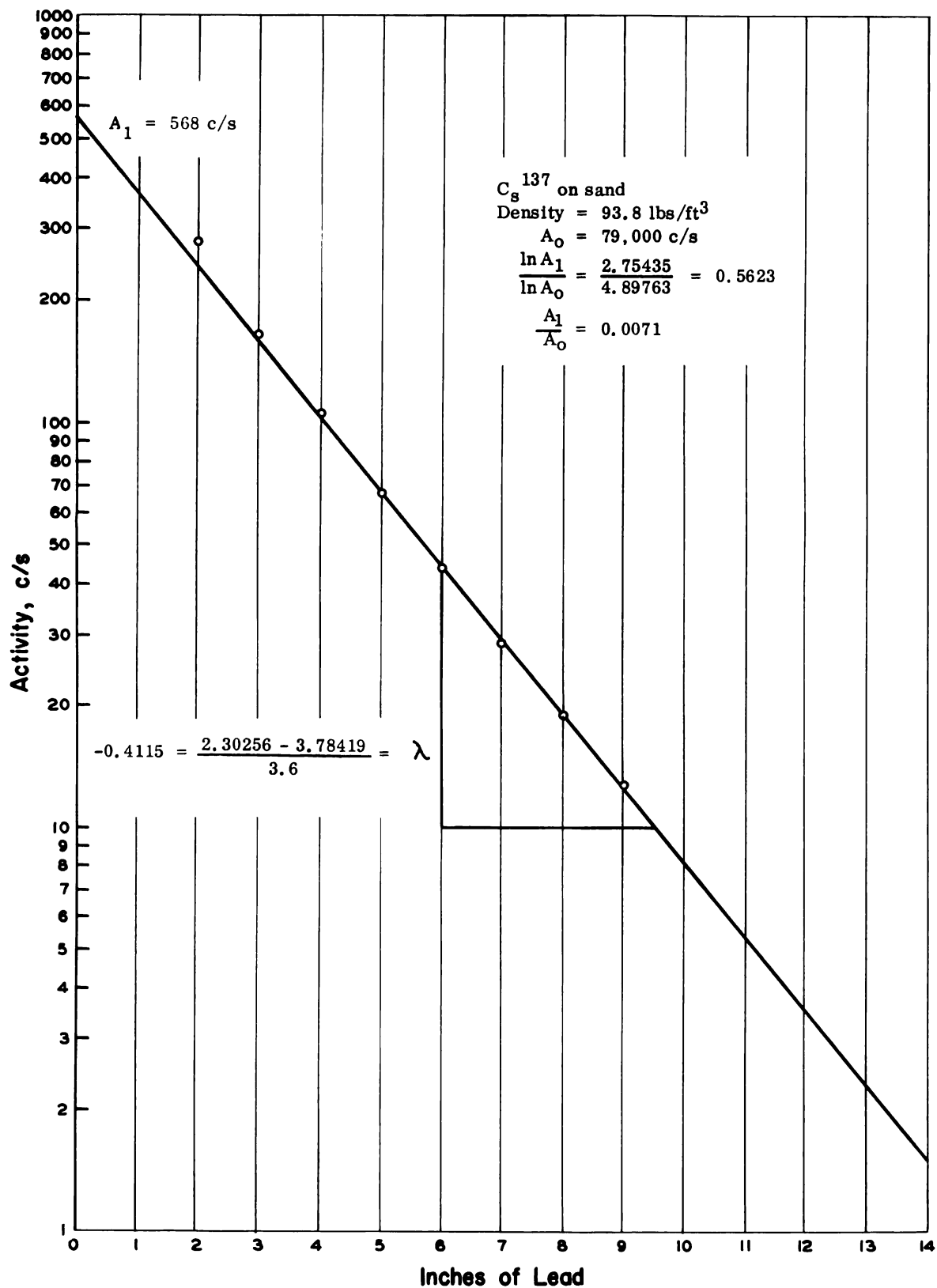
10. Goldberg, Irving; Trescony, Louis J.; Campbell, James S., Jr.; and Whyte, Gordon J.; Measurement of Moisture Content and Density of Soil Masses Using Radioactivity Methods. Paper prepared for presentation at the 1954 Pacific Coast Regional Conference on Clays and Clay Technology, June 25-6, 1954, University of California, Berkeley.
11. Horonjeff, Robert; Goldberg, Irving; and Trescony, Louis J.; The Use of Radioactive Material for the Measurement of Water Content and Density of Soil. Paper prepared for presentation at the Sixth Annual Street and Highway Conference, February 3-5, 1954, University of California, Los Angeles.
12. Evans, Robley D. The Atomic Nucleus. (p. 711) New York; McGraw-Hill Book Company, Inc., 1955. 972 pp.
13. Friedlander, Gerhart, and Joseph W. Kennedy. Introduction to Radiochemistry. (p. 170) New York: John Wiley & Sons, Inc., 1949. 412 pp.

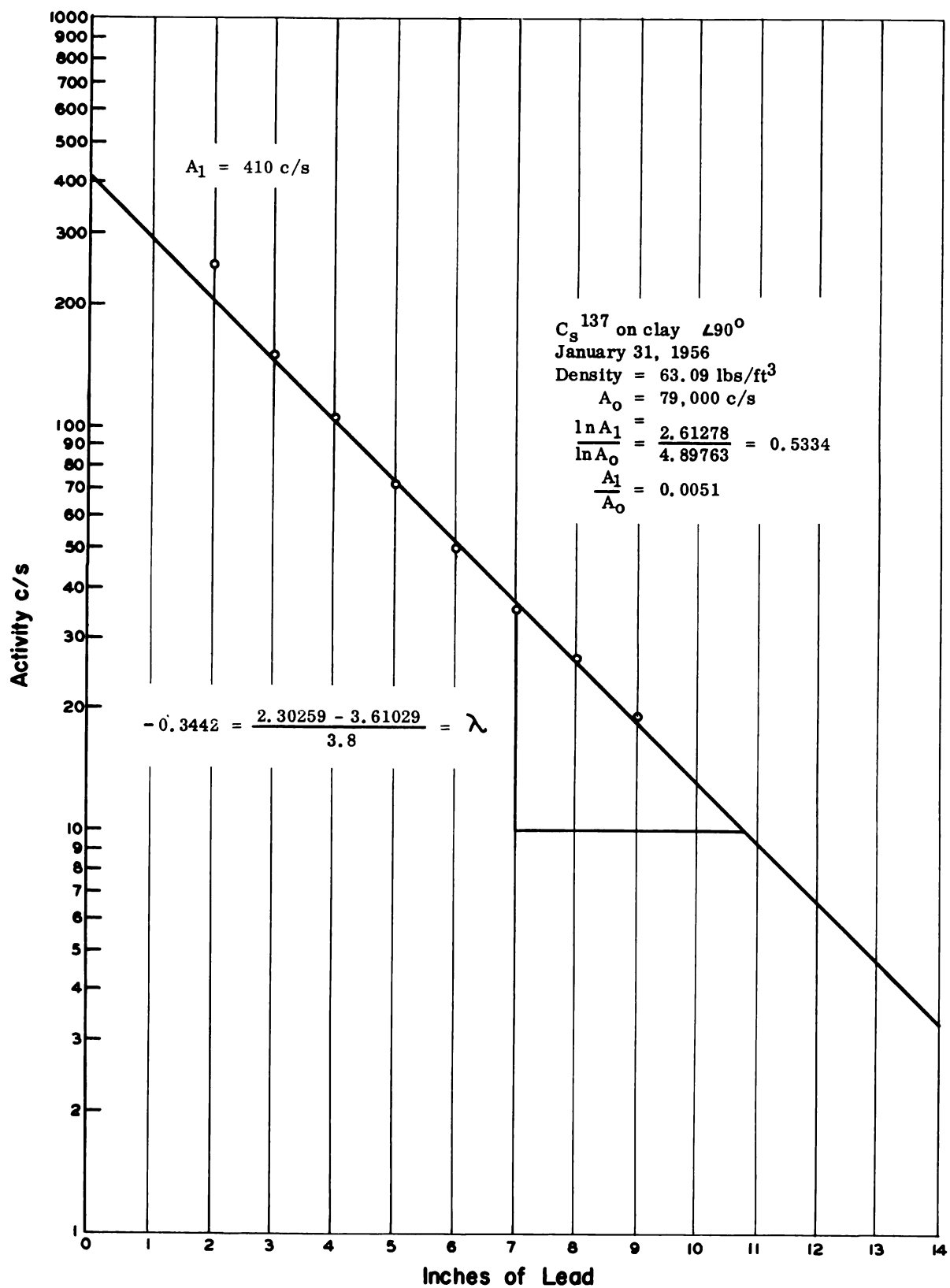
APPENDIXES

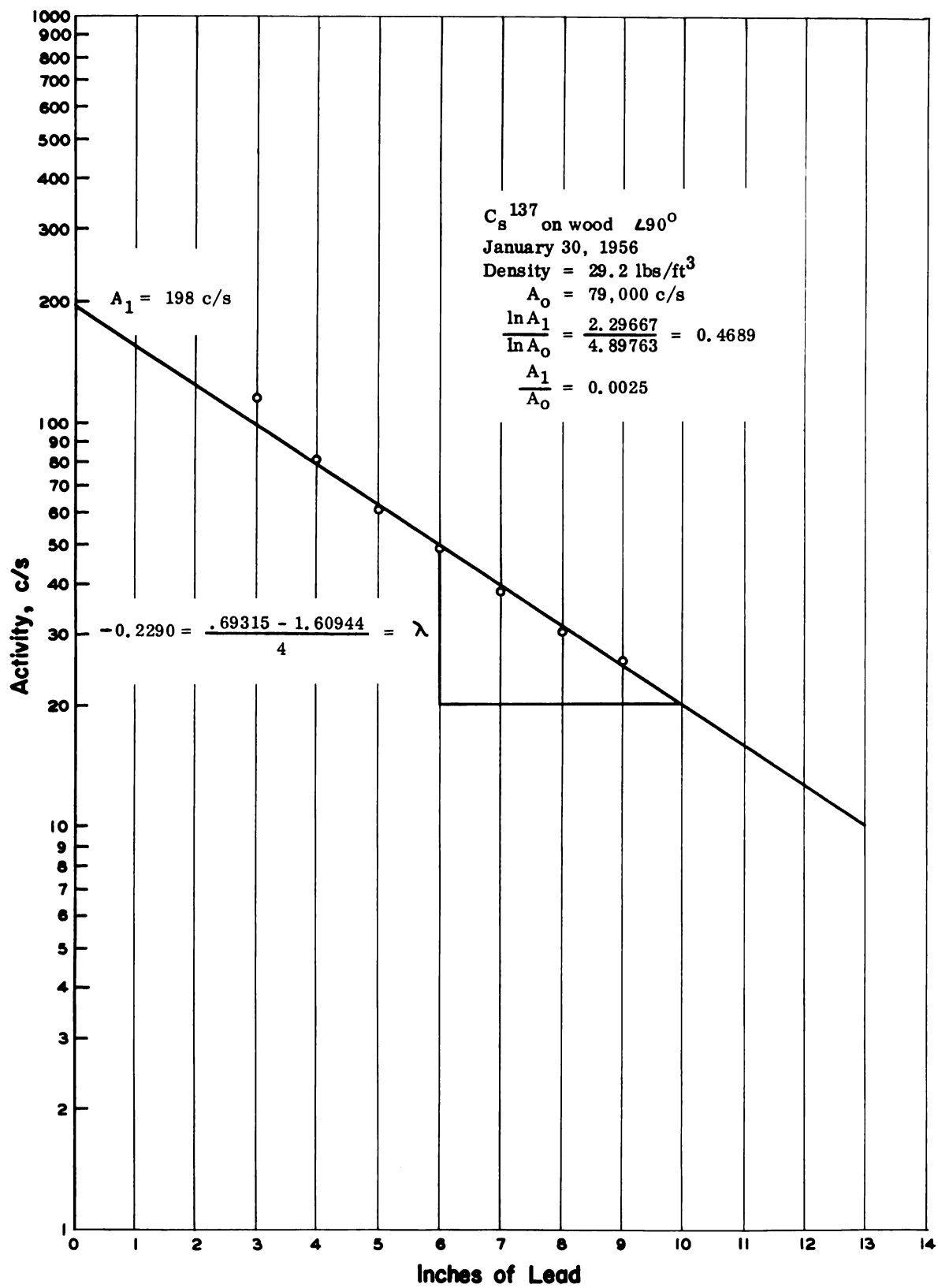
APPENDIX A

**GRAPHS FOR DETERMINATION OF f_1 AND f_2 FUNCTIONS
FOR CONCRETE, SAND, CLAY, AND WOOD SUBSTRATES**









APPENDIX B

DATA FOR DEVELOPMENT OF EMPIRICAL CALIBRATION CURVE

$$A_s = gA \frac{f_1(D)}{e} \frac{f_2(D)x}{e}$$

$$A = 79,000 \text{ c/s}$$

$$x = 6.0''$$

$$g = 1 \text{ (assumed)}$$

$$A_s = 79,000 \frac{f_1(D)}{e} \frac{f_2(D)(6)}{e} \text{ at } x = 6.0''$$

Using data from Figure 4,

D, #/ft ³	f ₁	f ₂	A _s	
			c/s	c/m
10	.429	-.1473	52.150	3129.0
20	.467	-.2025	57.481	3448.86
30	.4895	-.2436	57.892	3473.52
40	.506	-.2778	56.796	3407.76
50	.520	-.308	55.487	3329.22
60	.530	-.334	53.139	3188.34
70	.540	-.359	51.198	3071.88
80	.5494	-.380	50.184	3011.04
90	.5563	-.4011	47.7945	2867.67
100	.563	-.421	45.744	2744.64
110	.570	-.440	44.168	2650.08
120	.5765	-.458	42.662	2559.72
130	.5825	-.475	41.222	2473.32
140	.5868	-.4905	39.428	2365.68
150	.590	-.507	37.023	2221.38
160	.596	-.520	36.6425	2198.55
180	.6045	-.550	33.6857	2021.14
200	.611	-.5784	30.5684	1834.10
220	.619	-.604	28.6911	1721.47
250	.6285	-.640	25.7316	1543.90
300	.641	-.6955	21.2357	1274.14
400	.6648	-.7925	15.5193	931.16
500	.6813	-.879	11.1245	667.47

APPENDIX C

CHARACTERISTICS OF SOILS USED IN DEVELOPMENT OF EXPERIMENTAL CALIBRATION CURVE

GRAIN SIZE DISTRIBUTION

Sample	(%) Clay	(%) Silt	(%) Sand	Gravel
876	4	5	37	54
877	14	23	56	7
878	14.5	20	60.5	5
879	14	21	56	9
880	← Cinders →			
1 & 2	20	21	53	6
3 & 4	16	28	50	6
21 & 22	18	24	51	7

LEGEND FOR ABOVE TABLE

GRAIN SIZE

Clay	0.005 mm	to →
Silt	0.05 mm	to 0.005 mm
Sand	1.0 mm	to 0.05 mm
Gravel	→	to 1.0 mm

MOISTURE CONTENTS OF SOILS

Sample No.	Per Cent of Moisture		
	Dry Basis	Wet Basis	Difference
876	4.15	3.97	0.18
877	19.15	16.08	3.07
878	19.65	16.39	3.26
879	16.50	14.19	2.31
880	11.67	10.45	1.22
1	22.90	18.65	4.25
2	23.02	18.68	4.34
3	23.60	19.36	4.24
21	14.34	12.55	1.79
22	15.95	13.77	2.18

ATTERBERG CONSTANTS OF SOILS

No.	L. L.	P. L.	P. I.
876	-----	-----	-----
877	15.00	-----	0
878	16.20	-----	0
879	16.10	-----	0
880	-----	-----	-----
1 & 2	20.40	-----	0
3 & 4	20.0	-----	0
21 & 22	17.80	-----	0
20	28.92	23.20	5.7

ROOM USE ONLY

Date Due[illegible]

MICHIGAN STATE UNIVERSITY LIBRARIES



3 1293 03175 4868